Chapter 11
The Use of Nanomaterials in Electro-Fenton and Photoelectro-Fenton Processes

Ignasi Sirés and Enric Brillas

Abstract Nowadays, electro-Fenton and photoelectro-Fenton are considered two of the best electrochemical advanced oxidation processes to ensure fast degradation of organic pollutants and inactivation of toxic pathogens. Despite their apparent simplicity, two critical factors must be carefully controlled in order to enhance the production of $^{\bullet}OH$ from homogeneous Fenton's reaction: the H_2O_2 electrogeneration from cathodic O_2 reduction, and the characteristics of metal species employed to catalyze the quick decomposition of H_2O_2. In conventional electrochemical Fenton-based systems, the cathodes are made of either raw carbon powder or massive carbon pieces since these materials are known to promote the two-electron reduction of O_2 to yield H_2O_2, whereas Fe(II) or Fe(III) salts are added to allow homogeneous catalysis at optimum pH ~3. On the basis of this concept, good progress has been made when working with nanomaterials because the increased specific surface area provides: (i) more active cathode surfaces to produce H_2O_2; (ii) better heterogeneous catalysts, which may react to a larger extent with H_2O_2, within a wider pH range; (iii) a larger absorption of photons, promoting photoreduction and photooxidation reactions; and (iv) a larger area to adsorb pollutants that can be further degraded. As will be discussed in this chapter, most of the work has addressed the use of pristine, functionalized, and decorated nanocarbons as cathodes; the synthesis of nanocatalysts containing iron since this is the best metal for Fenton's reaction; and the preparation of nanostructured anodes.

Keywords Carbon felt · Carbon nanotubes · Electrochemical reactor · Gas diffusion · Graphene · Heterogeneous catalysis · Homogeneous catalysis · Hydrogen peroxide · Electro-Fenton · Nanomaterials · Photocatalysis · Photoelectro-Fenton · Surface functionalization · Water treatment

I. Sirés (✉) · E. Brillas
Laboratori d'Electroquímica dels Materials i del Medi Ambient, Departament de Química Física, Facultat de Química, Universitat de Barcelona, Barcelona, Spain
e-mail: i.sires@ub.edu

J. Filip et al. (eds.), *Advanced Nano-Bio Technologies for Water and Soil Treatment*, Applied Environmental Science and Engineering for a Sustainable Future,
https://doi.org/10.1007/978-3-030-29840-1_11

11.1 Introduction

The growing imbalance between water demand and water resources throughout the world, along with the scarcity of fresh water to sustain all human activities, has stimulated the development of a large variety of physical, chemical, photochemical, and electrochemical methods that show great efficiency in treating urban and industrial wastewater, aiming at its further reuse. The electro-Fenton (EF) process, initially called electrogenerated Fenton's reagent, was first used for wastewater treatment in the mid '80s (Brillas et al. 2009). EF is considered an electrochemical advanced oxidation process (EAOP) since it consists in the generation of homogeneous hydroxyl radical ($^{\bullet}OH$). This is achieved upon the occurrence of Fenton's reaction between Fe^{2+} and electrogenerated H_2O_2 (Brillas et al. 2009; Oturan and Aaron 2014; Sirés et al. 2014). $^{\bullet}OH$ is the second strongest oxidizing species known after fluorine, showing a large ability to mineralize most organic pollutants in water. The most characteristic feature of EF is that H_2O_2 is continuously dosed to the reaction medium from the two-electron reduction of O_2. This gas can be either directly fed as pure O_2 or air into the wastewater or pumped through a gas-diffusion device, further accepting the electrons typically supplied to a carbonaceous cathode. Thanks to the production of H_2O_2 on site, expensive and dangerous steps like industrial synthesis, transportation, storage, and handling can be avoided. Conventional homogeneous EF involves the addition of Fe^{2+} to the wastewater, although Fe^{3+} can be used alternatively because it is reduced to the former ion at the cathode surface (Oturan and Aaron 2014; Martínez-Huitle et al. 2015). The continuous Fe^{2+} and H_2O_2 (re)generation represents a significant advantage over the classical chemical Fenton process. In addition, the use of an undivided cell can accelerate the decontamination because of the production of heterogeneous M($^{\bullet}OH$) from water discharge at the surface of the anode M. On the other hand, one important drawback of EF when applied to organics removal is the production of Fe(III)-carboxylate complexes as final byproducts, which are quite refractory to $^{\bullet}OH$ attack. This phenomenon also occurs in the dark Fenton. To overcome this problem, the photoelectro-Fenton (PEF) process was developed in the mid '90s (Brillas et al. 2009). It consists in the simultaneous irradiation of the solution with artificial UV light or, more recently, sunlight, thus promoting the photolysis of intermediates like the Fe(III)-carboxylate species. As a result, a larger mineralization can be usually attained. The application of EF and PEF, along with the related processes, to the treatment of synthetic and real wastewater has been discussed in several authoritative reviews (Brillas et al. 2009; Oturan and Aaron 2014; Sirés et al. 2014; Martínez-Huitle et al. 2015; Moreira et al. 2017). Recently, the fundamentals, reactions, and applications of these EAOPs have been summarized in a comprehensive book edited by Zhou et al. (2018).

Other drawbacks of homogeneous EF and PEF include the limited pH range, i.e., ~3, to avoid the catalyst loss by precipitation, and the increase of soluble iron content in the treated effluent (Martínez-Huitle et al. 2015). Over the last decade, many efforts have been made to overcome such limitations, thus re-enforcing the EF and

PEF viability. Among the most valuable, nanoengineering has allowed the development of new nanomaterials as alternative cathodes, anodes, and catalysts. This chapter reviews the characteristics and applications of these materials, mainly prepared as: (i) cathodes to enhance the H_2O_2 electrogeneration and/or to promote heterogeneous Fenton's reaction, (ii) anodes to favor the electrocatalytic and photoelectrocatalytic production of $^{\bullet}OH$, and (iii) Fe-based catalysts to extend the pH range. Nanomaterials for hybrid treatments involving EF or PEF in combination with adsorption are described as well.

11.2 Nanomaterials as Cathodes

Many nanomaterials have been utilized to enhance the H_2O_2 production at the cathode of an electrolytic cell from the two-electron reduction of O_2 gas by reaction in Eq. 11.1. In some cases, they can simultaneously act as catalysts that favor the heterogeneous Fenton's reaction, mimicking the conventional Fenton's reaction (Eq. 11.2) with $^{\bullet}OH$ generation (Brillas et al. 2009; Oturan and Aaron 2014; Sirés et al. 2014; Martínez-Huitle et al. 2015; Moreira et al. 2017). The use of these modified cathodes is described in this section.

$$O_{2(g)} + 2H^+ + 2e^- \rightarrow H_2O_2 \tag{11.1}$$

$$Fe^{2+} + H_2O_2 \rightarrow Fe^{3+} + {}^{\bullet}OH + OH^- \tag{11.2}$$

11.2.1 Carbon-Based Nanomaterials

Carbonaceous materials are appealing targets to be used as catalysts for H_2O_2 electrogeneration since they are abundant, cheap, durable, and show good faradaic efficiency in the reaction in Eq. 11.1 (Čolić et al. 2018). A recent theoretical study by Chai et al. (2017) has reported that the reduction of O_2 molecules takes place by approaching the hydrogen sites on the carbon surface to form the hydroperoxide ion (HO_2^-), whose subsequent protonation yields H_2O_2. The two-electron oxygen reduction reaction (ORR) is then very effective in acidic media, which agrees with the optimum pH of conventional Fenton's reaction (Eq. 11.2), whereas in alkaline medium, the four-electron ORR to form H_2O prevails. The use of carbon-based nanomaterials allows increasing the electroactive surface area of the cathode, and consequently higher O_2 mass transport rates are achieved.

Carbon-based nanomaterials may exhibit outstanding electronic, photonic, electrocatalytic, chemical, and mechanical properties, depending on their nanoscale structure. Two main groups of materials can be distinguished: nanosized and nanostructured carbons (Khataee and Hasanzadeh 2017). The former is

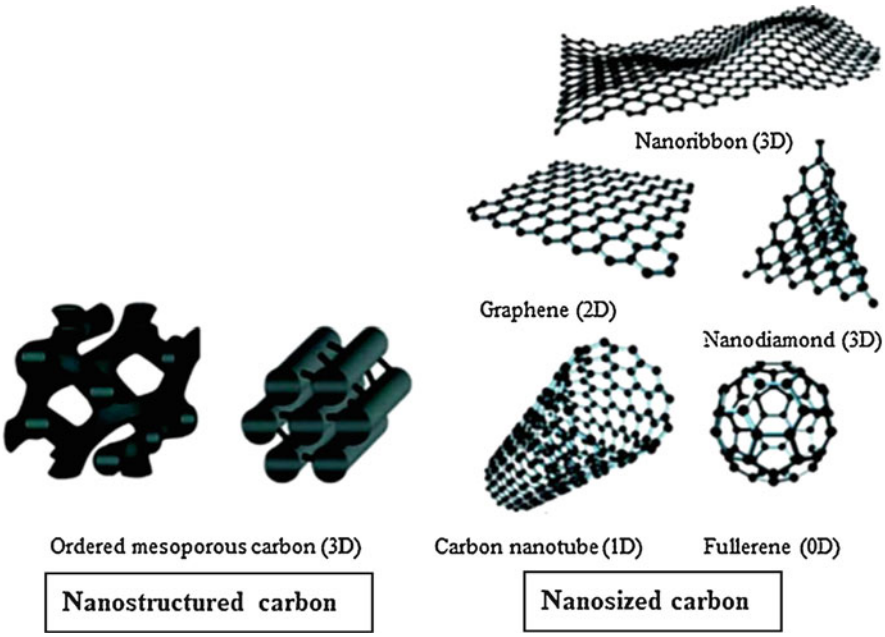

Fig. 11.1 Schematic illustration of some carbon-based nanomaterials. (Adapted from Khataee and Hasanzadeh (2017), Copyright 2017, with permission from Springer Nature)

characterized by nanometric shell size and thickness; and among others includes carbon nanotubes (CNTs), graphene (Gr) and its derivatives (graphene oxide (GO) and reduced graphene oxide (rGO)), nanofibers, nanodiamonds, nanocoils, nanoribbon, and fullerene. The latter group is composed of ordered mesoporous carbons and carbon fibers, which are constructed through various methodologies. Some examples of nanocarbons are shown in Fig. 11.1.

CNTs are ubiquitous carbon-based materials that allow the electrocatalysis of the reaction in Eq. 11.1. They have a hexagonal 1D structure with sp^2 hybridization (see Fig. 11.1), being formed upon the rolling up of a graphite layer that yields a nanoscale tube form (about 1 nm in diameter). The occurrence of two or more coaxial CNTs, with expanding diameters and tube separation of around 0.34 nm, gives rise to multi-walled CNTs (MWCNTs). CNTs sponge (Wang et al. 2014), classical CNTs (Khataee and Hasanzadeh 2017; Tian et al. 2016a), or MWCNTs (Roth et al. 2016) deposited onto gas-diffusion electrodes (GDEs), and graphite mixed with MWCNTs (Chu et al. 2013; Pajootan et al. 2014; Babaei-Sati and Parsa 2017) have been utilized to enhance the H_2O_2 generation, hence the removal of several organics by EF. For example, the Khataee's group reported that the amount of H_2O_2 produced using CNTs-based GDE was up to three-fold higher than using conventional GDE with activated carbon (Khataee and Hasanzadeh 2017). Wang et al. (2014) degraded 120 mL of 50 mg/L dimethyl phthalate in 0.1 M Na_2SO_4 with 0.5 mM Fe^{2+} at pH 3.0 by EF using an undivided cell with a Pt anode and either a

4 cm^2 CNTs sponge or graphite-based GDE as the cathode, at a cathodic potential (E_{cath}) of −0.50 V/saturated calomel electrode (SCE). After 120 min of electrolysis, the pollutant removal was 96% with 75% of total organic carbon (TOC) abatement using the sponge. These values are much higher than the 48% and 35% obtained for graphite-based GDE, respectively. A superior degradation performance upon the incorporation of CNTs in the GDE has also been described during the EF treatment of the dye Rhodamine B (Tian et al. 2016a). Excellent removal has also been reported for Acid Red 14 with a MWCNTs-based GDE (Roth et al. 2016) and for *m*-cresol (Chu et al. 2013), Basic Blue 41 (Pajootan et al. 2014), and Acid Red 14 and Acid Blue 92 (Babaei-Sati and Parsa 2017) with graphite-MWCNTs.

Graphene is composed of a 2D planar sheet with monoatomic thickness, made of sp^2 carbon atoms densely organized into a honeycomb structure (see Fig. 11.1). As in the case with CNTs, multilayers are also feasible. Graphene has been applied to the EF process as a pristine nanomaterial (Mousset et al. 2016b; Chen et al. 2016a), coated onto carbon felt (Le et al. 2015, 2017; Yang et al. 2017), carbon cloth (Mousset et al. 2016a), carbon-cloth GDEs (Garcia-Rodriguez et al. 2018), or carbon fiber (Mousset et al. 2017a), and mixed with graphite and PTFE (Zhang et al. 2018). Table 11.1 collects the main results obtained for several target organic pollutants using these cathodes. All the trials were carried out at bench scale using undivided cells at the optimum pH for Fenton's reaction (Eq. 11.2). Three-electrode cells with a constant E_{cath} between the cathode and the reference electrode (SCE) or two-electrode cells with constant current (I) or current density (j) were utilized.

In most cases, O_2 was bubbled into the solutions to ensure their saturation, aiming at enhancing the largest H_2O_2 production by the reaction in Eq. 11.1. In setups equipped with carbon cloth GDE (Garcia-Rodriguez et al. 2018), O_2 was pumped through the dry surface to produce H_2O_2 at the wet surface, which is in contact with the solution. Table 11.1 shows that very short electrolysis time was needed to degrade the model pollutants, whereas much longer time (up to 480 min) was necessary for achieving significant mineralization degrees because of the greater recalcitrance of byproducts to the attack of $^{\bullet}OH$. In general, worse results were found with raw cathodes without Gr. Figure 11.2 schematizes the preparation of a Gr/carbon-cloth cathode, involving the electrochemical exfoliation of a graphite rod to obtain graphene, which was mixed with Nafion® (PTFE suspension) and then ultrasonicated to obtain the graphene ink to coat the carbon cloth. Figure 11.2 also highlights the greater H_2O_2 electrogeneration with the Gr/carbon-cloth cathode compared with the uncoated cloth. This led to the greatest degradation (92%) and mineralization (57%) degrees for a 1.4 mM phenol solution using the coated cathode (see Table 11.1), only reaching 72% and 41% in the absence of Gr. Therefore, the larger H_2O_2 production favored a greater accumulation of $^{\bullet}OH$, thus resulting in the faster oxidation of organics.

Table 11.1 Selected results obtained for the EF treatment of several organic pollutants using undivided cells with cathodes based on graphene (Gr)

Cathode	Substrate	Experimental remarks	Best performance	Ref.
Gr	Phenol	150 mL of 1 mM substrate in 0.05 M K_2SO_4, 0.1 mM Fe^{2+}, pH 3.0, Pt anode, $E_{cath} = -0.60$ V/SCE	75% substrate decay (180 min), 49% TOC reduction (480 min)	Mousset et al. (2016b)
	Methylene Blue	100 mL of 11 mg/L dye in 0.1 mM Na_2SO_4, 11.1 mM Fe^{2+}, pH 3.0, Pt anode, $E_{cath} = -1.0$ V/SCE	100% color removal (160 min)	Chen et al. (2016a)
Gr/carbon felt	Acid Orange 7	30 mL of 0.1 mM dye in 0.05 M Na_2SO_4, 0.2 mM Fe^{2+}, pH 3.0, Pt anode, $I = 40$ mA	94% TOC removal (480 min)	Le et al. (2015)
	Orange II	100 mL of 50 mg/L dye in 0.05 M Na_2SO_4, 0.4 mM Fe^{2+}, pH 3.0, DSA® anode, $E_{cath} = -0.90$ V/SCE[e]	100% color and 79% TOC decays (60 min)	Yang et al. (2017)
Gr/carbon cloth[a]	Phenol	80 mL of 1.4 mM substrate in 0.05 M K_2SO_4, 0.1 mM Fe^{2+}, pH 3.0, Pt anode, $j = 1.25$ mA/cm^2	92% substrate decay (180 min), 57% TOC reduction (480 min)	Mousset et al. (2016a)
Gr/carbon cloth (GDE)[b]	Electronic wastewater	400 mL of wastewater with 53.5 mg/L TOC, 0.2 mM Fe^{2+}, pH 3.0, BDD anode. $j = 29$ mA/cm^2 [f]	92% TOC decay (180 min)	Garcia-Rodriguez et al. (2018)
Gr/carbon fiber[c]	Phenol	400 mL of 0.33 mM substrate in 0.05 M K_2SO_4, 0.1 mM Fe^{2+}, pH 3.0, Pt anode, $j = 1.25$ mA/cm^2	99% substrate decay (120 min), 98% TOC reduction (360 min)	Mousset et al. (2017a)
Gr@graphite[d]	Rhodamine B	50 mL of 20 mg/L dye in 0.05 M Na_2SO_4, 0.3 M Fe^{2+}, pH 3.0, DSA® anode, $j = 20$ mA/cm^2 [e]	100% color and 79% COD decays (60 min)[g]	Zhang et al. (2018)

Cathode area: [a]15, [b]20, [c]126, and [d]1.5 cm^2. [e]DSA®—dimensionally stable anode. [f]BDD—boron-doped diamond. [g]COD—chemical oxygen demand

11.2.2 Chemically Modified Carbonaceous Nanomaterials

The ability of carbonaceous cathodes to electrogenerate H_2O_2 from the reaction in Eq. 11.1 can be enhanced by chemically modifying their surface. Zhou et al. (2014) modified a graphite felt (GF) with pure ethanol, yielding a material (GF-A) with carbon nanoparticles of average diameter ca. 500 nm on the surface of the filaments. A second kind of modification employing 90:10 (v/v) ethanol/hydrazine hydrate mixtures yielded oxygen- and nitrogen-containing functional groups (GF-B), resulting in weaker hydrophobicity compared with GF and GF-A, thus favoring the H_2O_2 generation. Its accumulation increased in the sequence: GF (67 mg/L) < GF-A (110 mg/L) < GF-B (176 mg/L) upon electrolysis of 130 mL of an O_2-saturated 0.05 M Na_2SO_4 solution at pH 3.0 using a three-electrode cell at

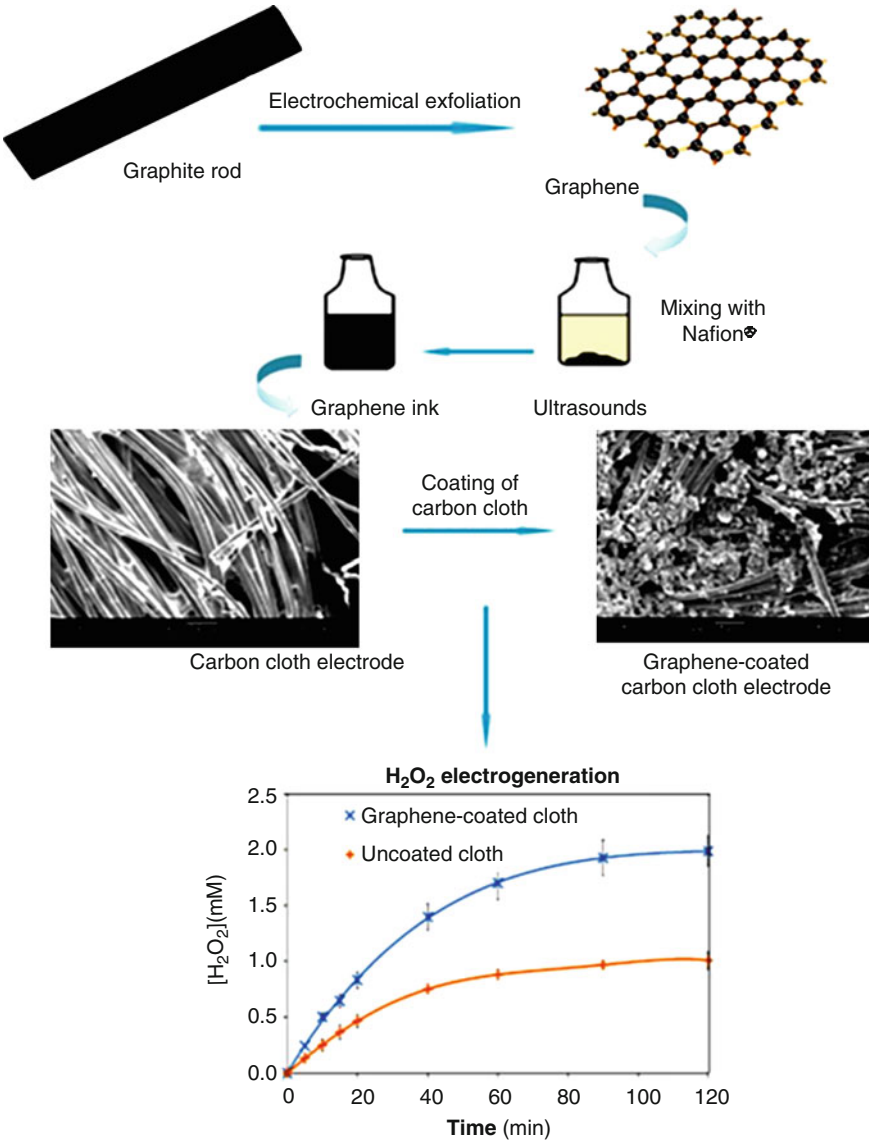

Fig. 11.2 Steps for the preparation of graphene-coated carbon cloth cathode. (Adapted from Khataee and Hasanzadeh (2017), Copyright 2017, with permission from Springer Nature). The graph represents the concentration of H_2O_2 accumulated in 80 mL of 0.05 M K_2SO_4 at pH 3.0 using an undivided cell with a Pt anode and uncoated or graphene-coated carbon cloth cathode, all with 15 cm^2 area, at current density of 1.25 mA/cm^2. (Adapted from Mousset et al. (2016a), Copyright 2016, with permission from Elsevier)

$E_{cath} = -0.65$ V/SCE for 120 min. The same trend was obtained when the performance of the EF process was assessed using 50 mg/L *p*-nitrophenol under the above conditions using 0.2 mM Fe^{3+} as catalyst, reaching 67%, 83%, and 99% substrate decay at 60 min and 22%, 32%, and 51% mineralization at 120 min with GF, GF-A, and GF-B, respectively. The superiority of GF-B containing N-doped carbon nanoparticles was related to the higher current recorded, which promoted the H_2O_2 production and the reduction of Fe^{3+} to Fe^{2+}, thereby increasing the amount of $^{\bullet}OH$ generated.

N-doping then favors the occurrence of the two-electron ORR to yield H_2O_2 since it increases the chemically active sites, the O_2 chemisorption, and the hydrophilicity of the carbon surface (Khataee and Hasanzadeh 2017). This has been confirmed for the other modified nanocarbons like N-CNTs (Zhang et al. 2008) and an N-Gr@CNTs composite GDE (Liu et al. 2016), which were used to treat 250 mL of Methyl Orange and 100 mL of 50 mg/L dimethyl phthalate solutions in 0.05 M Na_2SO_4 with 0.2–0.5 mM Fe^{2+} at pH 3.0 by EF using three-electrode undivided cells with a Pt anode at E_{cath} of -0.85 and -0.50 V/SCE, respectively. In the former system, 100% decolorization was obtained after 60 min using N-CNTs, a value higher than 82% found with an unmodified CNTs cathode. In the other case, the highest TOC removal of 52% at 180 min with the N-Gr@CNTs GDE was superior to 26%, 12%, 7.4%, and 38% reached with Gr@CNTs GDE, CNTs-based GDE, Gr-based GDE, and graphite-based GDE as the cathode, respectively. However, a contradictory interpretation of the behavior of the N-doped carbonaceous cathodes has been proposed in the recent work of Yang et al. (2018b). These authors prepared GF cathodes coated with Gr and N-Gr. Figure 11.3a and b evidence that the N-Gr particles deposited onto the graphite fibers were more uniform than the Gr ones. The degradation of 100 mL of 50 mg/L phenol in 0.05 M Na_2SO_4 at pH 3.0 with a DSA® anode at $E_{cath} = -0.90$ V/SCE revealed the removal of 99% and 78% phenol using GF with N-Gr and Gr within 50 min, respectively. This was ascribed to the formation of $^{\bullet}OH$ from the H_2O_2 reduction via the in situ metal-free processes illustrated in Fig. 11.3c, which was enhanced with the N-Gr-coated GF, as detected by ESR spectroscopy. Figure 11.3d shows phenol removal efficiency of 99% using the N-Gr-GF cathode at pH 3.0, quite similar to the 97% obtained using EF with Gr and 0.40 mM Fe^{2+}. At pH 7.0, phenol disappearance slowed down under the latter conditions, attaining 41%. When using N-Gr-GF without an iron catalyst, removal efficiency of up to 92% was achieved. These surprising results should be confirmed in future works, because such a large formation of $^{\bullet}OH$ from H_2O_2 reduction at GF coated with N-Gr is difficult to justify considering the state-of-the-art of EAOPs.

On the other hand, Quan and coauthors have recently developed hierarchically porous carbon (HPC) as a novel structure with a high electrocatalytic activity for the ORR to form H_2O_2. These materials are derived from the carbonization of metal–organic frameworks (MOFs), giving rise to abundant micro-, meso-, or even macropores with transference of C-sp^2 to C-sp^3 that can act as active sites for O_2 adsorption, eventually improving the kinetics of ORR (Liu et al. 2015b). F-doped HPC cathodes have been reported as good electrocatalysts for H_2O_2 generation (Zhao et al. 2018b). Liu et al. (2015a) prepared an HPC electrode from Zn^{2+} and

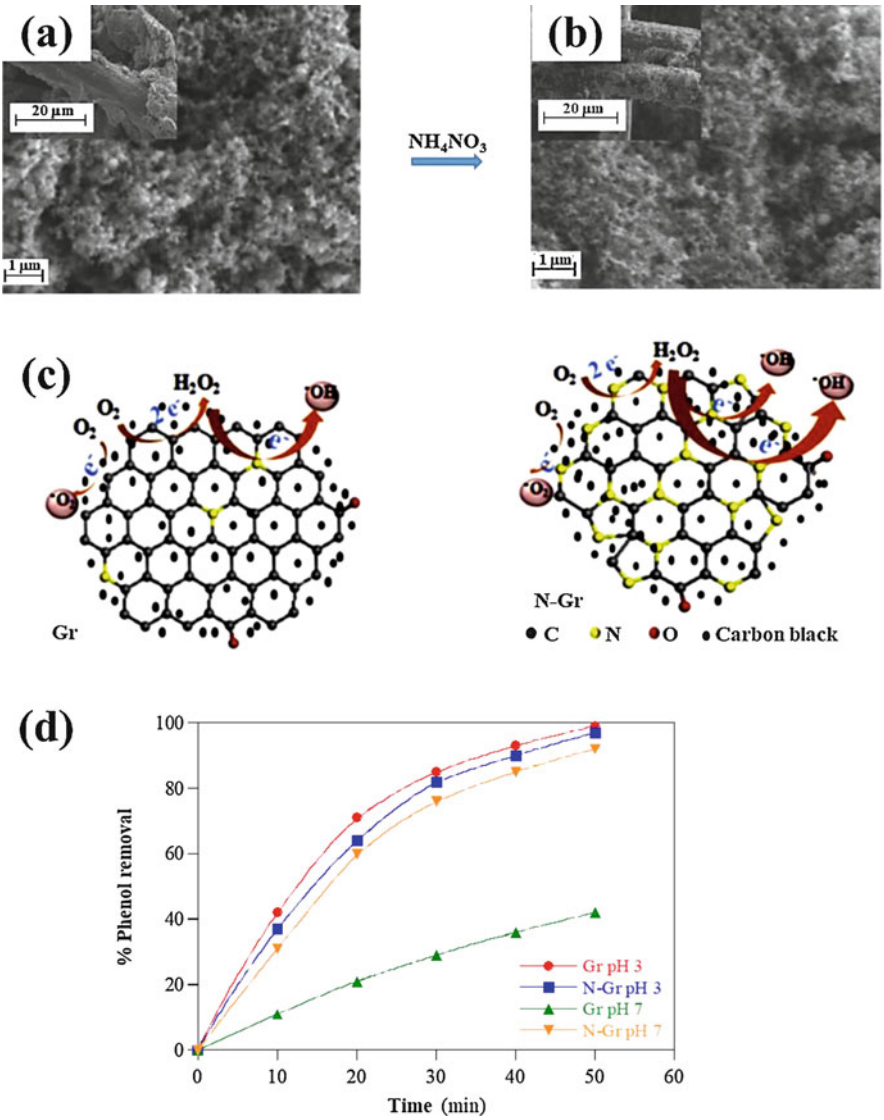

Fig. 11.3 SEM images of raw graphite-felt cathode modified with (**a**) graphene (Gr) and (**b**) N-doped graphene (N-Gr). (**c**) Schematic illustration of the in situ metal-free reactions occurring in the above cathodes. (**d**) Percentage of phenol removal during the treatment of 100 mL of 50 mg/L phenol in 0.05 M Na_2SO_4 using a cell with a DSA® anode and each of the above cathodes at $E_{cath} = -0.90$ V/SCE. The EF trials with Gr were made using 0.40 mM Fe^{2+}. No Fe^{2+} was added using N-Gr. (Adapted from Yang et al. (2018b), Copyright 2018, with permission from Elsevier)

1,4-benzenedicarboxylic acid as precursors, carrying out the carbonization under H_2 atmosphere. This electrode was used as the cathode of a three-electrode undivided cell with a Pt anode, yielding 97% of substrate decay and 91% TOC abatement after

180 and 240 min, respectively, upon EF treatment of 50 mg/L of perfluorooctanoate in 0.05 M Na_2SO_4 with 1.0 mM Fe^{2+} at pH 2.0 and $E_{cath} = -0.40$ V/SCE.

11.2.3 Non-Ferrous Metal-Modified Carbon Nanomaterials

For a given cathode material, the H_2O_2 production can be maximized by optimizing main experimental parameters like the electrolyte composition, pH, temperature, cell configuration, and applied current or E_{cath} (Yang et al. 2018a). Recently, the modification of carbonaceous cathodes with nonferrous metals has been addressed aiming at improving their electroactivity, i.e., trying to cause the ORR at less negative potential in order to reach higher current values at lower overvoltage. In this scenario, several authors have reported a large H_2O_2 enhancement by using Au-Pd (Pizzutilo et al. 2017) and Pt-Hg (Siahrostami et al. 2013) nanoparticles immobilized onto glassy carbon (GC). However, only few papers have described the use of bimetallic nanomaterials for the EF treatment of wastewater. For example, Félix-Navarro et al. (2013) deposited bimetallic Pt-Pd nanoparticles on MWCNTs, which were sprayed onto a reticulated vitreous carbon (RVC) GDE. This cathode allowed the accumulation of 71 mM H_2O_2 in 20 mL of 0.5 M H_2SO_4 after 20 min at $E_{cath} = -0.50$ V vs. Ag/AgCl. This was much greater than 2.2 mM obtained with a similar cathode without nanoparticles, as a result of the great electroactive area of Pt-Pd nanoparticles. Under these conditions, nitrobenzene was rapidly and completely degraded by EF with 0.1 mM Fe^{2+}.

Other authors have used metallic oxide nanoparticles, such as TaO_2 deposited onto GDE (Carneiro et al. 2016), $WO_{2.72}$ mixed with Vulcan carbon to prepare GDEs (Paz et al. 2018), and $Ce_xA_{1-x}O_2$ (A = Zr, Cu, or Ni) immobilized onto carbon felt (Li et al. 2017), to enhance the electroactivity regarding the H_2O_2 production. The use of $WO_{2.72}$@Vulcan GDE and Pt as the cathode and anode in a three-electrode cell to degrade 350 mL of a 0.260 mM Orange II solution in 0.1 M K_2SO_4 with 0.50 mM Fe^{2+} at pH 3.0 by EF yielded 100% decolorization after 120 min at $E_{cath} = -0.70$ V vs Ag/AgCl. This potential was selected because it led to the maximum H_2O_2 accumulation (i.e., 480 mg/L) in the absence of a catalyst (Paz et al. 2018). The crucial role of $^{\bullet}OH$ formed from Fenton's reaction (Eq. 11.2) was confirmed from the poorer color loss, ca. 20%, achieved under analogous conditions but without Fe^{2+}. In that so-called electrochemical oxidation with electrogenerated H_2O_2 (EO-H_2O_2) process, heterogeneous Pt($^{\bullet}OH$) is formed from water discharge from the reaction in Eq. 11.3 (Brillas et al. 2009; Oturan and Aaron 2014; Sirés et al. 2014; Martínez-Huitle et al. 2015; Moreira et al. 2017). In EF, both $^{\bullet}OH$ and Pt($^{\bullet}OH$) contribute to the dye oxidation, with predominance of the former radical.

$$Pt + H_2O \rightarrow Pt(^{\bullet}OH) + H^+ + e^- \qquad (11.3)$$

Co and Co-based materials also possess excellent characteristics for H_2O_2 electrogeneration in EF and PEF. Barros et al. prepared a GDE modified with 5% Co-phthalocyanine for the EF treatment of 400 mL of solutions containing 100 mg/L of the food dyes Amaranth (Barros et al. 2014b) and Tartrazine (Barros et al. 2014a), with 0.1 M K_2SO_4 and 0.15 mM Fe^{2+} at pH 2.5, using a three-electrode undivided cell with a Pt anode at $E_{cath} = -0.70$ V vs. Ag/AgCl. After 90 min, 79% and 98% decolorization, with 67% and 75% TOC removal, related to 370 and 219 kWh per kg TOC removed, were obtained, respectively. Ridruejo et al. (2018) showed the viability of a CoS_2/MWCNTs GDE cathode to degrade 150 mL of 0.112 mM of the anaesthetic tetracaine in 0.05 M Na_2SO_4 at pH 3.0 in a two-electrode cell with a BDD anode at $j = 100$ mA/cm^2. The authors found the complete drug disappearance at 120 and 60 min of EO-H_2O_2 and PEF with a 6 W UVA lamp, respectively, with TOC reductions of 43% and 60% at 180 min. The superiority of PEF was explained by the generation of $^{\bullet}OH$ from Fenton's reaction (Eq. 11.2) and the photoreduction of photoactive $Fe(OH)^{2+}$ via the reaction in Eq. 11.4, along with the photodecomposition of final Fe(III)-carboxylate species ($Fe(OOCR)^{2+}$) via the reaction in Eq. 11.5:

$$Fe(OH)^{2+} + h\nu \rightarrow Fe^{2+} + {}^{\bullet}OH \tag{11.4}$$

$$Fe(OOCR)^{2+} + h\nu \rightarrow Fe^{2+} + CO_2 + R^{\bullet} \tag{11.5}$$

What is also worth highlighting, Liang et al. (2016, 2017) proposed a heterogeneous EF-like treatment to decolorize 100 mL of 50 mg/L of Methyl Orange in 0.05 M Na_2SO_4 at pH 3–9 in a two-electrode undivided cell, with a Ti/IrO_2-RuO_2 anode (DSA®) and a cathode composed of GDE or GF coated with Co, at $j = 5$ mA/cm^2. A large H_2O_2 accumulation (about 595 mg/L) was obtained in the background electrolytes after 120 min of electrolysis, whereas 100% and 86% decolorization of the dye solution was attained after 180 min at pH 3.0 and pH 9.0, respectively, using coatings with 1.0–1.5 wt.% Co. The cathodes presented a great stability, with <4% of loss of color removal after ten cycles. The authors also showed the formation of $^{\bullet}OH$, which was ascribed to the Fenton-like reaction (Eq. 11.6) between Co^{2+} and H_2O_2 at the cathode surface. The Co^{3+} ion formed was further reduced to Co^{2+}.

$$Co^{2+} + H_2O_2 \rightarrow Co^{3+} + {}^{\bullet}OH + OH^{-} \tag{11.6}$$

11.2.4 Fe-Loaded Carbon Nanomaterials

During the twenty-first century, many research efforts have been made to develop heterogeneous electro-Fenton (hetero-EF) and photoelectro-Fenton (hetero-PEF) processes using carbonaceous materials loaded with nanoparticles of Fe (Li et al. 2011; Bañuelos et al. 2015), Fe-Fe_2O_3 (Li et al. 2009; Ai et al. 2007; Ding et al.

2017), Fe_2O_3 (Wang et al. 2013; Peng et al. 2015; Sklari et al. 2015), FeOOH (Zhang et al. 2012, 2015a), Fe_3O_4 (Chen et al. 2016b; Tian et al. 2016b; Zhang et al. 2017), γ-Fe_2O_3/Fe_3O_4 (Plakas et al. 2016), Fe-Cu (Garrido-Ramírez et al. 2016; Zhao et al. 2016, 2018a), CoFe hydroxide (Ganiyu et al. 2017), and Fe_3S_4/Fe_7S_8 (Choe et al. 2018). In these processes, no soluble iron catalyst is added to the solution since Fenton's reaction (Eq. 11.2) occurs between Fe(II) adhered to the cathode surface and H_2O_2 produced at the same surface. Furthermore, leaching of iron ions from the catalyst can contribute to conventional homogeneous Fenton's reaction. The main aim when using heterogeneous catalysts is to make the application of water treatments without pH regulation feasible, i.e., at natural pH, which is usually circumneutral. These materials minimize the formation of iron hydroxide, with the consequent reduction of costs associated to sludge management. A potential drawback of such catalysts is their gradual solubilization upon the use and the reuse, which limits their lifetime, especially under acidic conditions. Therefore, it is crucial to test their stability in consecutive degradation cycles. Selected degradation and mineralization results for some organic pollutants treated by hetero-EF and hetero-PEF are summarized in Table 11.2. A good performance can be observed for both processes within the pH range 2–7, although it is slightly better at pH 3.0, which is in agreement with the optimum conditions of Fenton's reaction (Eq. 11.2). The data corroborate the viability of the heterogeneous treatments at neutral pH, showing acceptable effectiveness. A clear superiority of hetero-PEF over hetero-EF, leading to faster removal of the target pollutant and TOC, can also be observed under comparable conditions, which can be accounted for by the additional generation of $^{\bullet}OH$ from photoreaction (Eq. 11.4) and the photolysis of intermediates such as final Fe(III)-carboxylate complexes via the reaction in Eq. 11.5.

As an example, Fig. 11.4a shows that magnetite (Fe_3O_4) presents a relatively uniform and spherical shape, with an average diameter of 40–50 nm, whereas Fig. 11.4b confirms its successful loading on the activated carbon acting as GDE (Zhang et al. 2017). Figure 11.4c illustrates the hetero-EF mechanism proposed to destroy tetracycline upon the attack of different reactive oxygen species (ROS) including: (i) the superoxide radical ($O_2^{\bullet-}$) produced from O_2 via the reaction in Eq. 11.7, (ii) H_2O_2 formed from O_2 via the reaction in Eq. 11.1, and (iii) $^{\bullet}OH$ produced from heterogeneous Fenton's reaction (Eq. 11.8), with the subsequent reduction of Fe^{III} to Fe^{II} via the reaction in Eq. 11.9

$$O_{2(g)} + e^- \rightarrow O_2^{\bullet-} \tag{11.7}$$

$$\equiv Fe^{II} + H_2O_2 \rightarrow \equiv Fe^{III} + {}^{\bullet}OH + OH^- \tag{11.8}$$

$$\equiv Fe^{III} + e^- \rightarrow \equiv Fe^{II} \tag{11.9}$$

where ≡ means the Fe_3O_4 surface. On the other hand, Fig. 11.4d schematizes the generation of $^{\bullet}OH$ to attack Acid Orange 7, using a CoFe hydroxide/carbon felt cathode (Ganiyu et al. 2017). $^{\bullet}OH$ is formed homogeneously from the reactions in Eqs. 11.2 and 11.6 in acidic medium, owing to Fe^{2+} and Co^{2+} leaching from the

Table 11.2 Selected results obtained for the hetero-EF and hetero-PEF treatment of several organic pollutants using undivided cells with cathodes based on Fe-loaded carbon nanomaterials

Cathode	Pollutant	Experimental remarks	Best performance	Ref.
Hetero-EF treatment				
Fe/activated carbon	Methyl Orange	25 mL of 10 mg/L dye in 0.05 M Na_2SO_4, pH 3.0, Pt anode, $E_{cath} = -0.70$ V vs. Ag/AgCl	96% dye and 88% TOC decays (30 min)	Bañuelos et al. (2015)
Fe@Fe_2O_3/ACF[a]	Atrazine	30 mg/L herbicide in 0.05 M Na_2SO_4, pH 3.0, BDD anode, $I = 30$ mA	100% substrate decay (60 min), 87% TOC decay (240 min)	Ding et al. (2017)
Fe_2O_3/carbon aerogel[b]	Imidacloprid	100 mL of 200 mg/L insecticide in 0.1 M Na_2SO_4, pH 6.9, Pt anode, $j = 10$ mA/cm^2	69% insecticide decay (150 min)	Peng et al. (2015)
FeOOH/AC/GF	Aramanth[d]	300 mL of 80 mg/L dye in 0.2 M Na_2SO_4, pH 4.0, Pt anode, $E_{cath} = -0.64$ V/SCE	99% dye decay (210 min), 53% TOC removal (360 min)	Zhang et al. (2012)
Fe_3O_4/GDE	Tetracycline	100 mL of 50 mg/L drug in 0.05 M N_2SO_4, pH 3.0, Pt anode, $E_{cath} = -0.80$ V/SCE	100% drug, 65% COD, and 57% TOC reductions (120 min)	Zhang et al. (2017)
Fe-cu allophane/GC	Phenol	100 mL of 0.5 mM substrate in 0.05 M Na_2SO_4, pH 3.0 and 5.5, Pt anode, $E_{cath} = -0.60$ V vs. Ag/AgCl	100% substrate decay at 120 min (pH 3.0) and 240 min (pH 5.5)	Garrido-Ramírez et al. (2016)
CoFe hydroxide/carbon felt[c]	Acid Orange 7	300 mL of 0.1 mM dye in 0.05 M Na_2SO_4, pH 2.0–7.1, Pt anode, $j = 4.2$ mA/cm^2	100% color decay (10 min), 87% TOC dye (120 min) at pH 3.0	Ganiyu et al. (2017)
Hetero-PEF treatment				
Fe/activated carbon	Methyl Orange	25 mL of 10 mg/L dye in 0.05 M Na_2SO_4, pH 3.0, Pt anode, 75 mW/ cm^2 UVA, $E_{cath} = -0.70$ V vs. Ag/AgCl	100% dye and 98% TOC decays (30 min)	Bañuelos et al. (2015)
Fe_2O_3/carbon aerogel[b]	Imidacloprid	100 mL of 200 mg/L insecticide in 0.1 M Na_2SO_4, pH 6.9, Pt anode, 500 W Xe lamp, $j = 10$ mA/cm^2	95% substrate removal (150 min), 98% TOC decay (480 min)	Peng et al. (2015)

[a]ACF—activated carbon fiber. Cathode area: [b]3, and [c]4.5 cm^2. [d]Divided cell with 300 mL of catholyte and 100 mL of anolyte

cathode. In contrast, this radical originates from the heterogeneous reactions in Eqs. 11.10 and 11.11, with regeneration of the Fe^{II}/Co^{II}-OH catalyst and no metal release, at neutral pH.

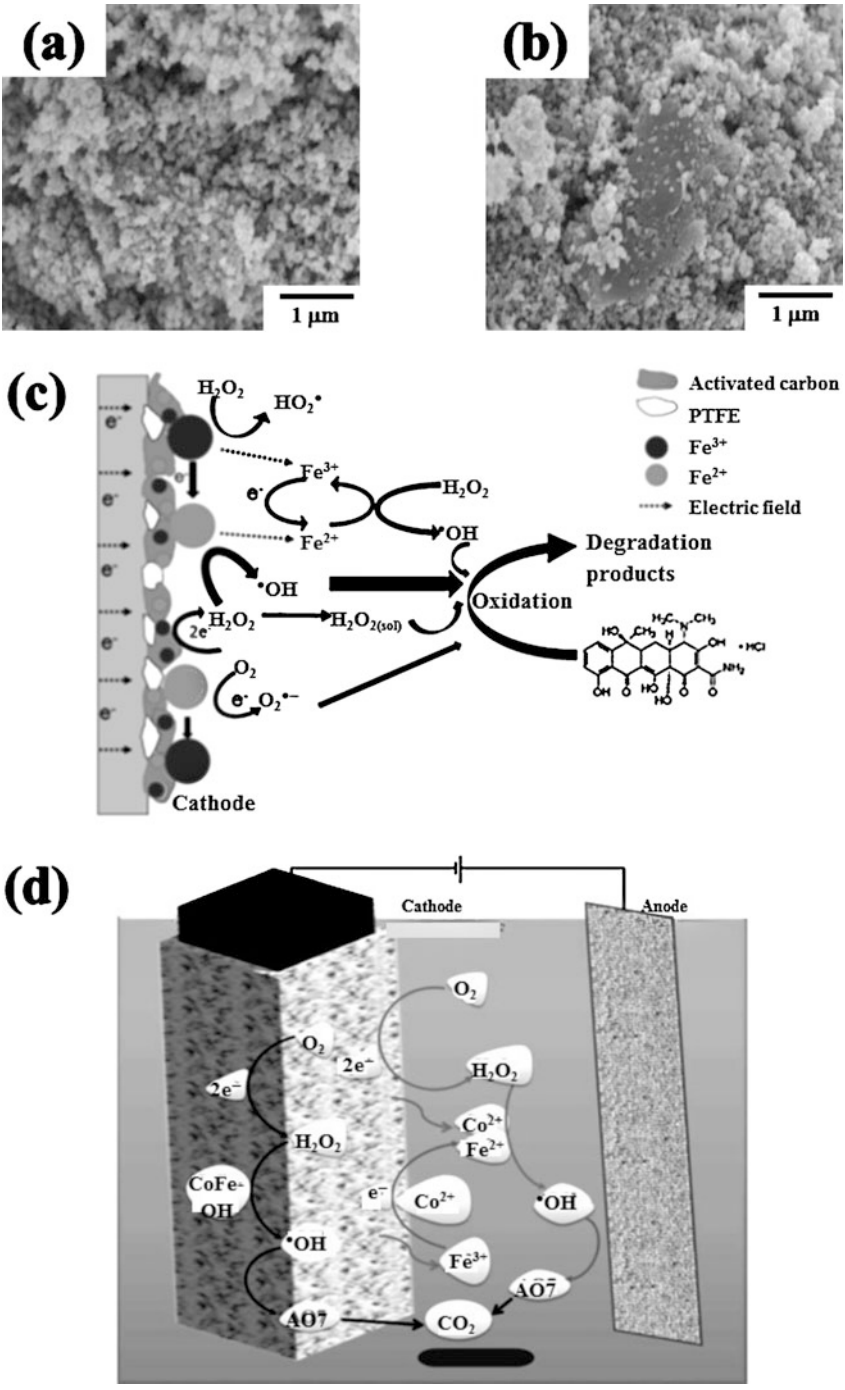

Fig. 11.4 SEM images of (**a**) pure Fe_3O_4 and (**b**) fresh Fe_3O_4/GDE. (**c**) Schematic illustration of the hetero-EF mechanism with the latter cathode. (Adapted from Zhang et al. (2017), Copyright 2017, with permission from Elsevier). (**d**) Schematic illustration of Acid Orange 7 (AO7) degradation in the hetero-EF system with a Pt anode and a CoFe–LDH/CF cathode). (Adapted from Ganiyu et al. (2017), Copyright 2017, with permission from The Royal Society of Chemistry)

$$\equiv Fe^{III}/Co^{III}\text{-}OH + H_2O_2 \rightarrow \equiv Fe^{II}/Co^{II}\text{-}OH + HO_2^{\bullet} + H^+ \quad (11.10)$$

$$\equiv Fe^{II}/Co^{II}\text{-}OH + H_2O_2 \rightarrow Fe^{III}/Co^{III}\text{-}OH + {}^{\bullet}OH + OH^- \quad (11.11)$$

11.3 Nanomaterials as Anodes

The EF and PEF treatments are usually carried out in cells equipped with conventional anodes like plates, rods/bars, or meshes. Alternatively, they can be performed with nanostructured anodes that can act as photoanodes or more efficient electrocatalysts. In the former case, hybrid processes with photoelectrocatalysis (PEC) have been devised. This section is focused on the preparation and application of such materials.

11.3.1 TiO_2-Based Photoanodes

The PEC method involves the use of a photoanode, commonly a nanocrystalline TiO_2-based material, in order to cause the light-induced oxidation of organic pollutants in aqueous media. This semiconductor has low cost and toxicity, and possesses a wide band gap of 3.2 eV (in the anatase form) (Garcia-Segura and Brillas 2017). Deposited as a thin film, it can absorb UV photons ($\lambda < 380$ nm) to promote an electron from the valence band to the conduction band (e^-_{CB}), with generation of a positively charged vacancy or hole (h^+_{VB}) via the reaction in Eq. 11.12. Organics can then be oxidized by: (i) the hole, (ii) heterogeneous ${}^{\bullet}OH$ formed from the reaction in Eq. 11.13 between h^+_{VB} and adsorbed water, and (iii) different ROS initiated from the reduction of O_2 by e^-_{CB} according to the reactions in Eqs. 11.14–11.17 (Sirés et al. 2014; Garcia-Segura and Brillas 2017).

$$TiO_2 + h\nu \rightarrow e^-_{CB} + h^+_{VB} \quad (11.12)$$

$$h^+_{VB} + H_2O \rightarrow {}^{\bullet}OH + H^+ \quad (11.13)$$

$$e^-_{CB} + O_2 \rightarrow O_2^{\bullet -} \quad (11.14)$$

$$O_2^{\bullet -} + H^+ \rightarrow HO_2^{\bullet} \quad (11.15)$$

$$2HO_2^{\bullet} \rightarrow H_2O_2 + O_2 \quad (11.16)$$

$$H_2O_2 + O_2^{\bullet -} \rightarrow {}^{\bullet}OH + OH^- + O_2 \quad (11.17)$$

The recombination of the e^-_{CB}/h^+_{VB} pair is the major drawback since it leads to significant efficiency loss. But this can be overcome by applying either an optimum constant I or a constant bias anodic potential (E_{anod}) to the illuminated photoanode (Brillas et al. 2009; Sirés et al. 2014; Garcia-Segura and Brillas 2017). This ensures the continuous extraction of photoinduced electrons, which are conveyed to the cathode through the external electrical circuit.

When a photoanode is combined with an appropriate carbonaceous cathode that electrogenerates H_2O_2 in the presence of Fe^{2+} as catalyst, the hybrid PEC/EF process takes place (Peralta-Hernández et al. 2006; Xie and Li 2006; Li et al. 2007; Esquivel et al. 2009; Ramírez et al. 2010; Ding et al. 2012, 2014; Lin et al. 2013; Almeida et al. 2014; Mousset et al. 2017b). In this case, only the photoanode is exposed to UV radiation. In contrast, if also the solution is illuminated, the process is the so-called PEC/PEF (Mousset et al. 2017b; Almeida et al. 2015). For example, Fig. 11.5a schematizes the formation of the main oxidant $^{\bullet}OH$ at a Bi_2WO_6 anode in PEC from the reaction in Eq. 11.13, which is combined with its formation via the reaction in Eq. 11.8 in hetero-PEF using an Fe@Fe_2O_3/activated carbon fiber (ACF) cathode. Both radicals are employed to destroy the dye Rhodamine B (Ding et al. 2012).

Good performance of PEC/EF and PEC/PEF processes for the removal of several organics can be observed in Table 11.3. Apart from TiO_2, other effective photocatalysts like Bi_2WO_6 (Ding et al. 2012) and Pt/TiO_2 NTs (Almeida et al. 2014; Mousset et al. 2017b) have been tested. Table 11.3 also evidences, as expected, greater efficiency of PEC/PEF when compared to PEC/EF for the treatment of a phenol solution under comparable conditions, which results from the acceleration of the oxidation process thanks to the contribution of the reactions in Eqs. 11.4 and 11.5 (Mousset et al. 2017b). In most of these works, classical anodes were comparatively tested to confirm the better performance of the hybrid treatments. In the case of hybrid PEC/EF, for example, Rhodamine B solutions were mineralized up to 94% in a cell equipped with a Bi_2WO_6 photoanode under 300 W tungsten halogen lamp irradiation and an Fe@ACF cathode (see Table 11.3). In contrast, only 78% and 14% mineralization were found by EF with Pt/Fe@Fe_2O_3 cell and PEC with Bi_2WO_6/Pt cell, respectively, under analogous conditions. The outperformance of PEC/EF was explained by: (i) better separation of e^-_{CB}/h^+_{VB} pairs, with accumulation of a larger amount of oxidant holes at the photoanode surface, and (ii) the additional injection of photoinduced electrons to the Fe@Fe_2O_3/ACF cathode, enhancing the H_2O_2 production and yielding greater quantities of $^{\bullet}OH$. On the other hand, Fig. 11.5b illustrates the better performance of PEC/PEF with Pt/TiO_2 NTs anode under 80 W UVA illumination and GDE as cathode, as compared to EF with a Pt/GDE cell and PEC with a Pt/TiO_2 NTs photoanode and GDE as cathode (without added Fe^{2+}) (Almeida et al. 2015). As can be seen, the TOC of an Orange G solution was reduced by 97%, 87%, and 80%, respectively, after 200 mA h/L of specific electrical consumption. The combined oxidation by

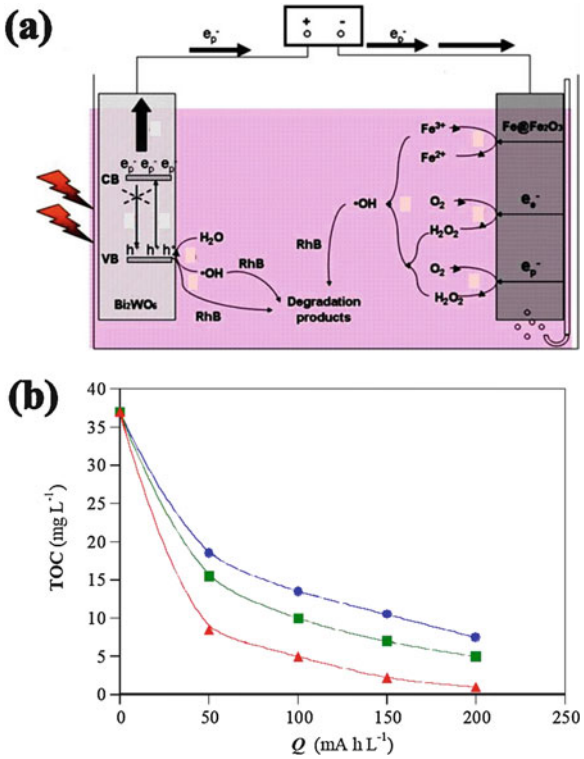

Fig. 11.5 (**a**) Schematic view of the main reactions to destroy Rhodamine B (RhB) by PEC with a Bi_2WO_6 photoanode combined with hetero-EF with a Fe@Fe_2O_3/ACF cathode. (Adapted from Ding et al. (2012), Copyright 2012, with permission of Elsevier). (**b**) Total organic carbon decay vs. applied electric charge for the (●) PEC, (■) EF, and (▲) PEC/PEF treatments of 500 mL of 85.4 mg/L Orange G solutions in 0.05 M Na_2SO_4 at pH 3.0. Anode in EF: Pt. Anode in PEC and PEC/PEF: Pt/TiO_2 NTs. Cathode: GDE. Applied current: 50 mA. Fe^{2+} concentration: 0.50 mM. Irradiation: 80 W UVA lamp. (Adapted from Almeida et al. (2015), Copyright 2015, with permission of Elsevier))

•OH formed from the reactions in Eqs. 11.2, 11.4, and 11.13, along with the photolytic action of UVA photons, accounts for the faster removal of organics by PEC/PEF.

As closely related to the aforementioned processes, the Khataee's group explored the characteristics of a PEF/photocatalysis treatment (Khataee et al. 2010, 2012, 2013, 2014; Zarei et al. 2010; Khataee and Zarei 2011), which can be considered as an alternative to the PEC/PEF system. Cubic undivided cells of 1.0–3.0 L capacity were equipped with the following elements: (i) a Pt anode, (ii) a CNTs-PTFE GDE as cathode fed with an O_2 flow, (iii) a 6 W UVA, UVB, or UVC lamp within a quartz tube, and (iv) four glass or ceramic plates coated with TiO_2 (Khataee et al. 2010, 2012, 2014; Zarei et al. 2010), N-doped TiO_2 (Khataee et al. 2013), or ZnO (Khataee and Zarei 2011) nanoparticles, which were placed covering the four inner cell walls.

Table 11.3 Selected results obtained for the PEC/EF and PEC/PEF treatment of several organics using undivided cells with nanostructured photoanodes

Photoanode, cathode	Substrate	Experimental remarks	Best performance	Ref.
PEC/EF treatment				
TiO_2/Ti, GF[a]	2,4-Dichlorophenol	50 mL of 15 mg/L substrate in 0.02 M Na_2SO_4, pH 3.0, 8 W UVA lamp, $I = 3.1$ mA	93% substrate and 78% TOC removal (60 min)	Li et al. (2007)
TiO_2/SS[b], graphite	Orange G	200 mL of 64 mg/L dye in 0.01 M Na_2SO_4, pH = 3.0, 330 μW/cm^2 UVA lamp, $E_{anod} = 1.0$ V/SCE	64% TOC removal (210 min)	Lin et al. (2013)
Bi_2WO_6, Fe@Fe_2O_3/ACF	Rhodamine B	100 mL of 10 μM dye in 0.05 M Na_2SO_4, pH 6.2, 300 W tungsten halogen lamp, $I = 0.3$ mA	94% TOC decay (240 min)	Ding et al. (2012)
Pt/TiO_2NTs, GDE	Acid Red 29	500 mL of 85.4 mg/L dye in 0.05 M Na_2SO_4, 0.50 mM Fe^{2+}, pH = 3.0, 80 W UVA lamp, $E_{anod} = 2.0$ V vs. Ag/AgCl	100% color removal (7 min), 98% TOC decay (200 mA h/L^{-1})	Almeida et al. (2014)
TiO_2/FTO[c], carbon felt	Phenol	200 mL of 1.4 mM substrate in 0.05 M K_2SO_4, 0.1 mM Fe^{2+}, pH = 3.0, 6 W UVA lamp, $I = 50$ mA	67% substrate decay (300 min), 76% TOC removal (480 min)	Mousset et al. (2017b)
PEC/PEF treatment				
TiO_2/FTO[c], carbon felt	Phenol	200 mL of 1.4 mM substrate in 0.05 M K_2SO_4, 0.1 mM Fe^{2+}, pH = 3.0, 6 W UVA lamp, $I = 50$ mA	100% substrate decay (300 min), 97% TOC removal (480 min)	Mousset et al. (2017b)
Pt/TiO_2NTs, GDE	Orange G	500 mL of 85.4 mg/L dye in 0.05 M Na_2SO_4, 0.50 mM Fe^{2+}, pH = 3.0, 80 W UVA lamp, $I = 50$ mA	100% color removal (30 min), 97% TOC decay (200 mA h/L)	Almeida et al. (2015)

[a]Second Fe anode at $I = 0.1$ mA as Fe^{2+} source. [b]SS—stainless steel, which acts as the source of an Fe^{2+} catalyst. [c]FTO—fluorine-doped tin oxide

Solutions of the dyes Acid Red 17 (Khataee et al. 2010), Basic Red 46 (Zarei et al. 2010), Acid Yellow 36 (Khataee et al. 2012), Direct Red 23 (Khataee et al. 2013), and Direct Yellow 12 (Khataee and Zarei 2011), as well as phenol (Khataee et al. 2014), in 0.05 M Na_2SO_4 with 0.1–0.2 mM Fe^{3+} at pH 3.0 were comparatively treated by the individual processes to show the benefits of the hybrid PEF/photocatalysis treatment. For example, for 2 L of 50 mg/L Direct Yellow 12 with 0.1 mM Fe^{3+} treated for 90 min at 100 mA under a 6 W UVC light irradiation (Khataee and Zarei 2011), the decolorization ability decreased as follows: PEF/photocatalysis (93%) > PEF (69%) > EF (56%), being much lower (39%) for photocatalysis alone (ZnO irradiated by UVC). The high mineralization power of the

PEF/photocatalysis method was shown by large TOC reduction (97%) achieved at 360 min. This can be attributed to the destruction of organics by: (i) heterogeneous Pt($^{\bullet}$OH) formed from the reaction in Eq. 11.3 and heterogeneous $^{\bullet}$OH from photogenerated holes on ZnO by the reaction in Eq. 11.13, (ii) homogeneous $^{\bullet}$OH formed from Fenton's reaction (Eq. 11.2), from photolysis of $Fe(OH)^{2+}$ species via the reaction in Eq. 11.4, and from UVC photolysis of electrogenerated H_2O_2, (iii) photoinduced holes produced on ZnO, similarly to the reaction in Eq. 11.12, and (iv) photodecomposition of intermediates under UVC radiation.

11.3.2 Electrocatalytic Anodes

Several authors have improved the EF method by synthesizing anodes with greater electrocatalytic ability as compared to conventional ones, thereby enhancing the production of heterogeneous $^{\bullet}$OH from water discharge, similarly to the reaction in Eq. 11.3. Examples of some stable, nanostructured anodes for such a purpose are β-PbO_2 (Sirés et al. 2010), porous Ni/BDD/Ta (Li et al. 2018), and ZnO-TiO_2/GF (El-Kacemi et al. 2017). The excellent performance of 3D β-PbO_2 deposits obtained from carbon/polyvinyl-ester composite (Sirés et al. 2010) for the EF process has been well proven for the treatment of 275 mL of an O_2-saturated solution with 0.25 mM Methyl Orange in 0.05 M Na_2SO_4 with 0.2 mM Fe^{2+} at pH 3.0, using an undivided glass cell with a carbon-felt cathode at $I = 60$ mA. Total decolorization was achieved after 60 min of electrolysis, a time shorter than 240 min needed for the analogous EO with Ni cathode in the absence of Fe^{2+}, at 300 mA. This corroborates much greater oxidation power of $^{\bullet}$OH formed from Fenton's reaction (Eq. 11.2) than PbO_2($^{\bullet}$OH) in EF. Further work of these authors showed the applicability of PbO_2 deposits onto RVC to EO (Recio et al. 2011; Ramírez et al. 2016), being feasible to incorporate TiNTs (Ramírez et al. 2016), which could be extended in the future to EF and PEF. Similarly, for 60 mg/L Methylene Blue in 0.05 M Na_2SO_4 at pH 3.0, the use of a porous Ni/BDD/Ta anode allowed the overall loss of color after 80 min of the EF treatment with 0.5 mM Fe^{2+} at 120 mA. This was faster than the comparable EO process, which required 240 min (Li et al. 2018). On the other hand, a nanostructured ZnO-TiO_2/GF anode was coupled to a GF cathode to treat 250 mL of an O_2-saturated solution with 0.12 mM of the dye Amido Black 10, 0.06 M Na_2SO_4, and 0.1 mM Fe^{2+} at pH 3.0 by EF at $I = 100$ mA (El-Kacemi et al. 2017). Under these conditions, the dye solution was completely decolorized in 60 min, whereas 91% mineralization was reached after 360 min of the treatment, showing good effectiveness of this anode for dye destruction.

11.4 Suspended Nanocatalysts

The synthesis of nanocatalysts to be suspended in solution, with the ability to form heterogeneous $^{\bullet}OH$ upon the reaction with electrogenerated H_2O_2, has widened the applicability of Fenton-based EAOPs for wastewater treatment through the development of hetero-EF and hetero-PEF. Similarly to what has been discussed in the case of Fe-loaded carbon nanomaterials used as cathodes, the main advantage of suspended nanocatalysts is that they allow operating within a larger pH range, and, therefore, neutralization of the final effluent may be avoided (Ganiyu et al. 2018; Poza-Nogueiras et al. 2018). This allows the minimization of sludge formation and prevents an excessive accumulation of iron ions in the treated effluent, which are common handicaps in the homogeneous processes. Moreover, the nanocatalyst is easy to handle, safe to store, it can be efficiently recovered and has the possibility of being reused (Ganiyu et al. 2018). As main drawbacks, suspended nanocatalysts may lose some of their active sites, thus reducing their catalytic ability, and they can undergo partial solubilization. This means that, on many occasions, there exists the conjunction of both homogeneous and heterogeneous processes during the treatment, even if this is disregarded by many authors.

A large number of nanomaterials has been synthesized and tested for hetero-EF, including: (i) Fe-based nanoparticles, like Fe_3O_4 (He et al. 2014; Es'haghzade et al. 2017), Pd/Fe_3O_4 (Luo et al. 2014; Huang et al. 2017), Fe molybdophosphate (Baiju et al. 2018), and zero-valent iron (Babuponnusami and Muthukumar 2012); (ii) Fe-carbon nanoparticles such as Fe-C/PTFE (Zhang et al. 2015b, c) and Fe_3O_4-CNTs (Shen et al. 2014); (iii) mineral-like nanocatalysts such as martite (Khataee et al. 2017); (iv) MOFs, only used in non-electrochemical systems so far, as described in detail in recent reviews (Dias and Petit 2015; Cheng et al. 2018); (v) supported Fe catalysts, such as Fe–zeolite (Rostamizadeh et al. 2018), Fe_3O_4–chitosan (Rezgui et al. 2018), Fe–silica (Jinisha et al. 2018), and Fe_2O_3–kaolin (Özcan et al. 2017); and (vi) non-Fe-based, like Cu/C (Xu et al. 2013). Table 11.4 collects selected results obtained in these works.

Successful degradations can be observed within the pH range 2–7, which confirms the viability of nanomaterials to operate at neutral pH—the condition required for the treatment of wastewater under real conditions.

In the case of Fe-based nanocatalysts, the proposed heterogeneous mechanism involves the oxidation of organics with heterogeneous $^{\bullet}OH$ produced via the reaction in Eq. 11.8, where H_2O_2 is generated at a suitable carbonaceous cathode (Ganiyu et al. 2018; Poza-Nogueiras et al. 2018). The regeneration of Fe^{II} at the catalyst surface can occur either by the reaction in Eq. 11.9, when the material comes into contact with the cathode upon stirring or recirculation, or by the heterogeneous Fenton-like reaction in Eq. 11.18.

$$\equiv Fe^{III} + H_2O_2 \rightarrow \equiv Fe^{II} + HO_2^{\bullet} + H^+ \qquad (11.18)$$

Table 11.4 Selected results obtained for the hetero-EF treatment of several organic pollutants using undivided cells with suspended nanostructured catalysts in solution

Nanocatalyst	Substrate	Experimental remarks	Best performance	Ref.
Fe_3O_4	Reactive Blue 19	200 mL of 100 mg/L dye in 0.05 M Na_2SO_4, 1 g/L catalyst, pH = 3.0, Fe/ACF cell, I = 120 mA	87% TOC removal (120 min)	He et al. (2014)
	Acid Red 14	250 mL of 50 mg/L substrate in 4 g/L Na_2SO_4, 0.6 g/L catalyst, pH = 7, graphite/graphite cell, I = 180 mA	92% (pH = 3), 83% (pH = 7), and 85% (pH = 9) color removal (120 min)	Es'haghzade et al. (2017)
Pd/Fe_3O_4	Humic acid + Cr(VI)	200 mL of 100 mg/L humic acid +20 mg/L Cr(VI), 1 g/L catalyst, pH = 3.0, BDD/Pt cell, I = 40 mA	90% TOC decay (480 min), total removal Cr (VI) (120 min)	Huang et al. (2017)
Zero-valent iron	Phenol	1 L of 200 mg/L substrate, 0.5 g/L catalyst, 500 mg/L H_2O_2, pH = 6.2, SS/SS cell, I = 60 mA	88% substrate decay (60 min)	Babuponnusami and Muthukumar (2012)
Fe-C/PTFE	2,4-Dichlorophenol	150 mL of 120 mg/L substrate in 0.05 M Na_2SO_4, 6 g/L catalyst, pH = 6.7, Ti/IrO_2-RuO_2/GDE cell, I = 100 mA	97% substrate and 34% TOC removals (120 min)	Zhang et al. (2015b)
Fe_3O_4/CNTs	Methylene Blue	150 mL of 0.24 mM dye in 0.10 M Na_2SO_4, 10 g/L catalyst, Ti/SnO_2/graphite cell, E_{cell} = 5 V [a]	70% (pH = 3), 73% (pH = 7), and 44% (pH = 9) color decay (30 min)	Shen et al. (2014)
Martite	Paraquat	100 mL of 20 mg/L herbicide in 0.05 M Na_2SO_4, 1 g/L catalyst, pH = 6, Pt/graphite cell, I = 300 mA	86% herbicide decay (150 min)	Khataee et al. (2017)
Fe–zeolite	Reactive Red 120	200 mL of 10 mg/L herbicide in 0.05 M Na_2SO_4, 1 g/L catalyst, pH = 3, graphite/graphite cell, I = 100 mA	94% color removal (30 min)	Rostamizadeh et al. (2018)
Fe_3O_4–chitosan	Chlordimeform	30 mL of 37.5 mg/L insecticide in 0.05 M Na_2SO_4, 0.5 g/L	100% insecticide decay (30 min),	Rezgui et al. (2018)

(continued)

Table 11.4 (continued)

Nanocatalyst	Substrate	Experimental remarks	Best performance	Ref.
		catalyst, pH = 3, Pt/carbon felt cell, I = 100 mA	80% TOC decay (360 min)	
Fe–silica	Rhodamine B	750 mL of 10 mg/L drug in 20 mg/ L Na_2SO_4, 15 mg/L catalyst, pH = 2, graphite/graphite cell, E_{cell} = 8 V	98% color and 35% TOC removals (180 min)	Jinisha et al. (2018)
Fe_2O_3–kaolin	Enoxacin	175 mL of 0.25 mM drug in 0.05 M Na_2SO_4, 0.3 g/L catalyst, pH = 5.1, Pt/carbon felt cell, I = 100 mA	100% drug removal (15 min), 99% TOC decay (360 min)	Özcan et al. (2017)
Cu/C	Phenol	200 mL of 2 mg/L substrate in 0.01 M Na_2SO_4, 1 g/L catalyst, 10 mg/L Fe^{2+}, pH = 3, Pt/Pt cell, I = 50 mA	80% (pH = 3) and 50% (pH = 5 and 7) substrate removals (180 min)	Xu et al. (2013)

[a] E_{cell}—potential difference between anode and cathode

Some authors have suggested more complex reaction mechanisms for hetero-EF when H_2O_2 is not cathodically produced. Figure 11.6a schematizes the steps proposed for the removal of humic acids (HAs) and Cr(VI) in a BDD/Pt cell using Pd/Fe_3O_4 as catalyst (Huang et al. 2017). These include: (i) H_2 and O_2 gas generation at the cathode and anode, respectively, (ii) diffusion of O_2 to the Pd/Fe_3O_4 nanoparticles to be reduced to the oxidant $O_2^{\bullet-}$, (iii) H_2O_2 formation from the reaction between H_2 and O_2 at the catalyst surface, (iv) generation of heterogeneous $^{\bullet}OH$ from heterogeneous Fenton's reaction (Eq. 11.8) between Fe^{II} at the Pd/Fe_3O_4 surface and produced H_2O_2, with subsequent Fe^{II} regeneration via the reaction in Eq. 11.9, and (v) $^{\bullet}OH$ formation at the BDD surface from a reaction similar to the one in Eq. 11.3. HAs are then oxidized by $O_2^{\bullet-}$ and $^{\bullet}OH$. According to step 6 shown in Fig. 11.6a, Cr(VI) is reduced to Cr(III) at the cathode, and by atomic H at the nanocatalyst surface, whereas as shown in step 7, Cr(III) can be removed upon the deposition of chromite ($FeCr_2O_4$). Similarly, for the treatment of phenol solutions with Cu/C nanoparticles (Xu et al. 2013), the H_2O_2 production from the heterogeneous reaction of H_2 and O_2 gases at the catalyst surface has been suggested. Hence, the oxidant $^{\bullet}OH$ is formed homogeneously from Fenton's reaction (Eq. 11.2) thanks to the addition of Fe^{2+} ion to the solution.

Several authors have also compared the homogeneous EF and hetero-EF treatments to show the excellent performance of the latter method. Figure 11.6b illustrates the normalized TOC abatement from a 0.25 mM enoxacin solution at pH 3.0 by homogeneous EF with 0.3 mM Fe^{2+} and hetero-EF with 0.1 g of Fe_2O_3–kaolin

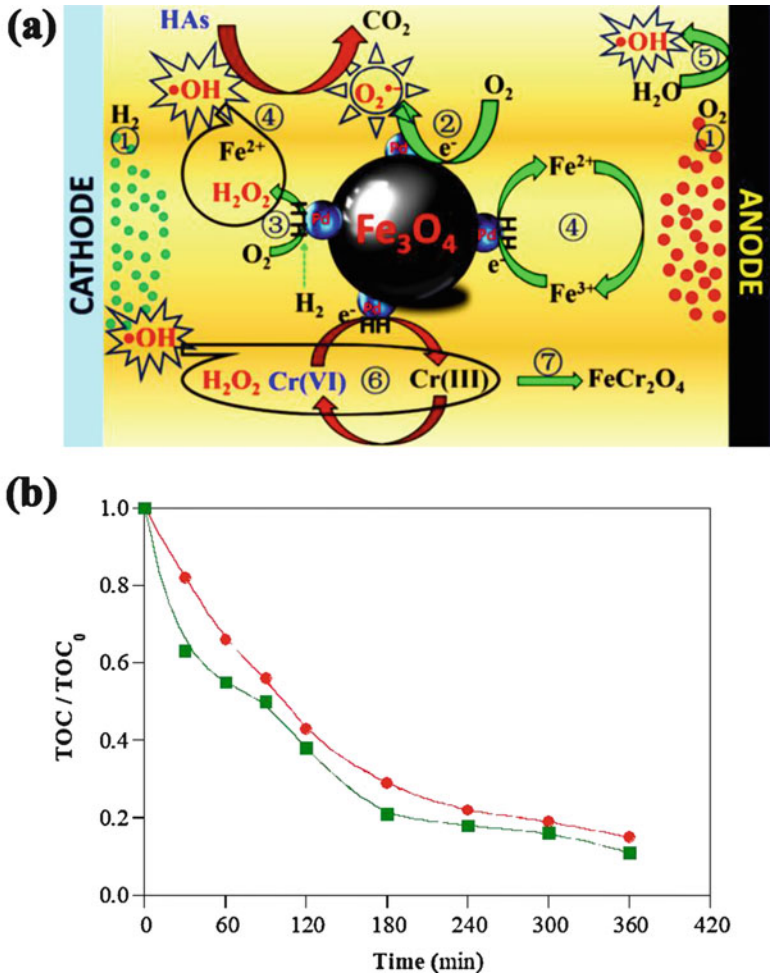

Fig. 11.6 **(a)** Schematic mechanisms for the removal of humic acid (HAs) and Cr(VI) by hetero-EF process with a BDD/Pt cell using Pd/Fe_3O_4 as catalyst. (Adapted from Huang et al. (2017), Copyright 2017, with permission from Elsevier). **(b)** Normalized TOC removal with electrolysis time for the treatment of 175 mL of 0.25 mM of the antibiotic enoxacin in 0.05 M Na_2SO_4 at pH 3.0 by (●) homogeneous EF with 0.30 mM Fe^{2+} and (■) hetero-EF with 0.1 g of Fe_2O_3–kaolin using a Pt/carbon felt cell. Applied current: 60 mA. (Adapted from Özcan et al. (2017), Copyright 2017, with permission from Elsevier)

using a Pt/carbon felt cell at 60 mA. After 360 min of electrolysis, 85% and 89% mineralization, respectively, was achieved, indicating the high effectiveness of the nanocatalyst, even superior to that of Fe^{2+} for $^{\bullet}OH$ generation. This should further encourage the research into novel nanomaterials with a higher catalytic activity and great stability for practical wastewater treatment, aiming to implement hetero-EF at industrial scale.

11.5 Nanomaterials in Hybrid Processes

Some other hybrid processes have been described to upgrade the oxidation ability of the EF and PEF methods (Brillas and Sirés 2018). However, the use of nanomaterials is rather limited to date, mainly being reduced to different kinds of carbon materials as adsorbents. Recently, Zhao et al. (2017) proposed a hybrid method involving electrosorption/EF to treat 100 mL of an O_2-saturated solution with 50 mg/L dimethyl phthalate in 0.05 M Na_2SO_4 at natural pH 6 using an undivided cell with a Pt anode and an Fe-doped carbon aerogel with Gr sheets as cathode at $I = 135$ mA. It was found that about 90% of the substrate was adsorbed on the cathode surface, whereas 98% of it was removed after 150 min of hetero-EF. The authors suggested a degradation mechanism involving the destruction of physisorbed dimethyl phthalate with heterogeneous $^{\bullet}OH$ formed from the reaction in Eq. 11.8. Wang et al. (2018) synthesized nanomaterials like $La_{1-x}Nd_xFeO_3$@activated carbon as anodes with a high adsorption ability. In only 10 min of EF treatment of Methyl Orange at pH 2.0 using GDE as cathode at $I = 60$ min, 99% color and 97% chemical oxygen demand (COD) was found, attaining 17% and 36% removal of such by direct adsorption at the same time. Direct removal of the adsorbed dye by heterogeneous $^{\bullet}OH$ formed from water oxidation at the anode and homogeneous $^{\bullet}OH$ from Fenton's reaction (Eq. 11.2) between the anodically leached Fe^{2+} and the produced H_2O_2 was proposed as the main degradation mechanism.

11.6 Conclusions

This chapter has reviewed the main current developments in the synthesis, modification, use, and reuse of key nanomaterials that enhance the performance of EF and PEF processes for the removal of organic pollutants from water. Since Fenton's reaction relies on the decomposition of H_2O_2 upon the reaction with Fe(II) to produce large amounts of $^{\bullet}OH$ in the bulk solution, efforts are particularly concentrated on new Fe-based nanocatalysts. We believe that research should especially focus on nanomaterials used as suspended catalysts since catalysts supported on the carbonaceous cathode surface tend to be detrimental for the two-electron ORR, and they may affect the material's stability and diminish the exposed carbon surface area for H_2O_2 electrogeneration. Investigation into potential Fe-based catalysts should pay special attention to their robustness, reducing the iron leaching to ensure a minimum secondary contamination and a greater reusability with reproducible performance. The use of MOFs in heterogeneous electrochemical Fenton-based EAOPs is forecast as a relevant topic in the near future. Novel cathodes, particularly those based on non-metal and non-ferrous nanocatalysts, may become the material of choice to electrogenerate H_2O_2 on site, and new electrode configurations might contribute to a significant improvement of such in situ electrosynthesis. The preparation of all these mentioned catalysts should, hopefully, be based on green synthesis

principles, as shown in the case of 3D PbO_2 electrodeposited using biocompatible methanesulfonic acid. Regarding the use of nanomaterials in hybrid processes, adsorption with nanomaterials like Gr followed by EF or PEF post-treatments of the resulting effluents is an interesting way worth exploring, which can be combined with washing nanoadsorbents by means of Fenton-based EAOPs, as recently addressed by some authors. Finally, it is worth mentioning that the tests of these new materials and reactors should be carried out with real wastewater matrices in order to correctly assess their viability when compared to robust separation technologies like adsorption, (electro)coagulation, or membrane separation. Reusability tests in those complex matrices are thus needed to assess the impact of the catalyst degradation on the treatment costs as well as the reproducibility upon successive usage.

References

Ai Z, Mei T, Liu J, Li J, Jia F, Zhang L, Qiu J (2007) Fe@Fe_2O_3 core–shell nanowires as an iron reagent. 3. Their combination with CNTs as an effective oxygen-fed gas diffusion electrode in a neutral electro-Fenton system. J Phys Chem C 111(40):14799–14803. https://doi.org/10.1021/jp073617c

Almeida LC, Silva BF, Zanoni MVB (2014) Combined photoelectrocatalytic/electro-Fenton process using a Pt/TiO_2NTs photoanode for enhanced degradation of an azo dye: a mechanistic study. J Electroanal Chem 734:43–52. https://doi.org/10.1016/j.jelechem.2014.09.035

Almeida LC, Silva BF, Zanoni MVB (2015) Photoelectrocatalytic/photoelectro-Fenton coupling system using a nanostructured photoanode for the oxidation of a textile dye: kinetics study and oxidation pathway. Chemosphere 136:63–71. https://doi.org/10.1016/j.chemosphere.2015.04.042

Babaei-Sati R, Parsa JB (2017) Electrogeneration of H_2O_2 using graphite cathode modified with electrochemically synthesized polypyrrole/MWCNT nanocomposite for electro-Fenton process. J Ind Eng Chem 52:270–276. https://doi.org/10.1016/j.jiec.2017.03.056

Babuponnusami A, Muthukumar K (2012) Removal of phenol by heterogenous photo electro Fenton-like process using nano-zero valent iron. Sep Purif Technol 98:130–135. https://doi.org/10.1016/j.seppur.2012.04.034

Baiju A, Gandhimathi R, Ramesh ST, Nidheesh PV (2018) Combined heterogeneous electro-Fenton and biological process for the treatment of stabilized landfill leachate. J Environ Manag 210:328–337. https://doi.org/10.1016/j.jenvman.2018.01.019

Bañuelos JA, García-Rodríguez O, Rodríguez-Valadez FJ, Godínez LA (2015) Electrochemically prepared iron-modified activated carbon electrodes for their application in electro-Fenton and photoelectro-Fenton processes. J Electrochem Soc 162(9):E154–E159. https://doi.org/10.1149/2.0581509jes

Barros WRP, Alves SA, Franco PC, Steter JR, Rocha RS, Lanza MRV (2014a) Electrochemical degradation of tartrazine dye in aqueous solution using a modified gas diffusion electrode. J Electrochem Soc 161(9):H438–H442. https://doi.org/10.1149/2.015409jes

Barros WRP, Franco PC, Steter JR, Rocha RS, Lanza MRV (2014b) Electro-Fenton degradation of the food dye amaranth using a gas diffusion electrode modified with cobalt (II) phthalocyanine. J Electroanal Chem 722–723:46–53. https://doi.org/10.1016/j.jelechem.2014.03.027

Brillas E, Sirés I (2018) Chapter 11 - Hybrid and sequential chemical and electrochemical processes for water decontamination. In: Martínez-Huitle CA, Rodrigo MA, Scialdone O (eds)

Electrochemical water and wastewater treatment. Butterworth-Heinemann, Oxford, pp 267–304. https://doi.org/10.1016/B978-0-12-813160-2.00011-0

Brillas E, Sirés I, Oturan MA (2009) Electro-Fenton process and related electrochemical technologies based on Fenton's reaction chemistry. Chem Rev 109(12):6570–6631. https://doi.org/10.1021/cr900136g

Carneiro JF, Rocha RS, Hammer P, Bertazzoli R, Lanza MRV (2016) Hydrogen peroxide electrogeneration in gas diffusion electrode nanostructured with Ta_2O_5. Appl Catal A 517:161–167. https://doi.org/10.1016/j.apcata.2016.03.013

Chai G-L, Hou Z, Ikeda T, Terakura K (2017) Two-electron oxygen reduction on carbon materials catalysts: mechanisms and active sites. J Phys Chem C 121(27):14524–14533. https://doi.org/10.1021/acs.jpcc.7b04959

Chen C-Y, Tang C, Wang H-F, Chen C-M, Zhang X, Huang X, Zhang Q (2016a) Oxygen reduction reaction on graphene in an electro-Fenton system: in situ generation of H_2O_2 for the oxidation of organic compounds. ChemSusChem 9(10):1194–1199. https://doi.org/10.1002/cssc.201600030

Chen W, Yang X, Huang J, Zhu Y, Zhou Y, Yao Y, Li C (2016b) Iron oxide containing graphene/carbon nanotube based carbon aerogel as an efficient E-Fenton cathode for the degradation of methyl blue. Electrochim Acta 200:75–83. https://doi.org/10.1016/j.electacta.2016.03.044

Cheng M, Lai C, Liu Y, Zeng G, Huang D, Zhang C, Qin L, Hu L, Zhou C, Xiong W (2018) Metal-organic frameworks for highly efficient heterogeneous Fenton-like catalysis. Coord Chem Rev 368:80–92. https://doi.org/10.1016/j.ccr.2018.04.012

Choe YJ, Byun JY, Kim SH, Kim J (2018) Fe_3S_4/Fe_7S_8-promoted degradation of phenol via heterogeneous, catalytic H_2O_2 scission mediated by S-modified surface Fe^{2+} species. Appl Catal B 233:272–280. https://doi.org/10.1016/j.apcatb.2018.03.110

Chu Y, Zhang D, Liu L, Qian Y, Li L (2013) Electrochemical degradation of *m*-cresol using porous carbon-nanotube-containing cathode and Ti/SnO_2–Sb_2O_5–IrO_2 anode: kinetics, byproducts and biodegradability. J Hazard Mater 252–253:306–312. https://doi.org/10.1016/j.jhazmat.2013.03.018

Čolić V, Yang S, Révay Z, Stephens IEL, Chorkendorff I (2018) Carbon catalysts for electrochemical hydrogen peroxide production in acidic media. Electrochim Acta 272:192–202. https://doi.org/10.1016/j.electacta.2018.03.170

Dias EM, Petit C (2015) Towards the use of metal–organic frameworks for water reuse: a review of the recent advances in the field of organic pollutants removal and degradation and the next steps in the field. J Mater Chem A 3(45):22484–22506. https://doi.org/10.1039/C5TA05440K

Ding X, Ai Z, Zhang L (2012) Design of a visible light driven photo-electrochemical/electro-Fenton coupling oxidation system for wastewater treatment. J Hazard Mater 239–240:233–240. https://doi.org/10.1016/j.jhazmat.2012.08.070

Ding X, Ai Z, Zhang L (2014) A dual-cell wastewater treatment system with combining anodic visible light driven photoelectro-catalytic oxidation and cathodic electro-Fenton oxidation. Sep Purif Technol 125:103–110. https://doi.org/10.1016/j.seppur.2014.01.046

Ding X, Wang S, Shen W, Mu Y, Wang L, Chen H, Zhang L (2017) Fe@Fe_2O_3 promoted electrochemical mineralization of atrazine via a triazinon ring opening mechanism. Water Res 112:9–18. https://doi.org/10.1016/j.watres.2017.01.024

El-Kacemi S, Zazou H, Oturan N, Dietze M, Hamdani M, Es-Souni M, Oturan MA (2017) Nanostructured ZnO-TiO_2 thin film oxide as anode material in electrooxidation of organic pollutants. Application to the removal of dye Amido black 10B from water. Environ Sci Pollut Res 24(2):1442–1449. https://doi.org/10.1007/s11356-016-7920-6

Es'haghzade Z, Pajootan E, Bahrami H, Arami M (2017) Facile synthesis of Fe_3O_4 nanoparticles via aqueous based electro chemical route for heterogeneous electro-Fenton removal of azo dyes. J Taiwan Inst Chem Eng 71:91–105. https://doi.org/10.1016/j.jtice.2016.11.015

Esquivel K, Arriaga LG, Rodríguez FJ, Martínez L, Godínez LA (2009) Development of a TiO_2 modified optical fiber electrode and its incorporation into a photoelectrochemical reactor for wastewater treatment. Water Res 43(14):3593–3603. https://doi.org/10.1016/j.watres.2009.05.035

Félix-Navarro RM, Beltrán-Gastélum M, Salazar-Gastélum MI, Silva-Carrillo C, Reynoso-Soto EA, Pérez-Sicairos S, Lin SW, Paraguay-Delgado F, Alonso-Núñez G (2013) Pt–Pd bimetallic nanoparticles on MWCNTs: catalyst for hydrogen peroxide electrosynthesis. J Nanopart Res 15:1802. https://doi.org/10.1007/s11051-013-1802-3

Ganiyu SO, Le TXH, Bechelany M, Esposito G, van Hullebusch ED, Oturan MA, Cretin M (2017) A hierarchical CoFe-layered double hydroxide modified carbon-felt cathode for heterogeneous electro-Fenton process. J Mater Chem A 5(7):3655–3666. https://doi.org/10.1039/C6TA09100H

Ganiyu SO, Zhou M, Martínez-Huitle CA (2018) Heterogeneous electro-Fenton and photoelectro-Fenton processes: a critical review of fundamental principles and application for water/wastewater treatment. Appl Catal B 235:103–129. https://doi.org/10.1016/j.apcatb.2018.04.044

Garcia-Rodriguez O, Lee YY, Olvera-Vargas H, Deng F, Wang Z, Lefebvre O (2018) Mineralization of electronic wastewater by electro-Fenton with an enhanced graphene-based gas diffusion cathode. Electrochim Acta 276:12–20. https://doi.org/10.1016/j.electacta.2018.04.076

Garcia-Segura S, Brillas E (2017) Applied photoelectrocatalysis on the degradation of organic pollutants in wastewaters. J Photochem Photobiol C 31:1–35. https://doi.org/10.1016/j.jphotochemrev.2017.01.005

Garrido-Ramírez EG, Marco JF, Escalona N, Ureta-Zañartu MS (2016) Preparation and characterization of bimetallic Fe–Cu allophane nanoclays and their activity in the phenol oxidation by heterogeneous electro-Fenton reaction. Microporous Mesoporous Mater 225:303–311. https://doi.org/10.1016/j.micromeso.2016.01.013

He Z, Gao C, Qian M, Shi Y, Chen J, Song S (2014) Electro-Fenton process catalyzed by Fe_3O_4 magnetic nanoparticles for degradation of C.I. reactive blue 19 in aqueous solution: operating conditions, influence, and mechanism. Ind Eng Chem Res 53(9):3435–3447. https://doi.org/10.1021/ie403947b

Huang B, Qi C, Yang Z, Guo Q, Chen W, Zeng G, Lei C (2017) Pd/Fe_3O_4 nanocatalysts for highly effective and simultaneous removal of humic acids and Cr(VI) by electro-Fenton with H_2O_2 *in situ* electro-generated on the catalyst surface. J Catal 352:337–350. https://doi.org/10.1016/j.jcat.2017.06.004

Jinisha R, Gandhimathi R, Ramesh ST, Nidheesh PV, Velmathi S (2018) Removal of rhodamine B dye from aqueous solution by electro-Fenton process using iron-doped mesoporous silica as a heterogeneous catalyst. Chemosphere 200:446–454. https://doi.org/10.1016/j.chemosphere.2018.02.117

Khataee A, Hasanzadeh A (2017) Modified cathodes with carbon-based nanomaterials for electro-Fenton process. In: Zhou M, Oturan MA, Sirés I (eds) Electro-Fenton process: new trends and scale-up. Springer, Singapore, pp 111–143. https://doi.org/10.1007/698_2017_74

Khataee AR, Zarei M (2011) Photocatalysis of a dye solution using immobilized ZnO nanoparticles combined with photoelectrochemical process. Desalination 273(2–3):453–460. https://doi.org/10.1016/j.desal.2011.01.066

Khataee AR, Zarei M, Asl SK (2010) Photocatalytic treatment of a dye solution using immobilized TiO_2 nanoparticles combined with photoelectro-Fenton process: optimization of operational parameters. J Electroanal Chem 648(2):143–150. https://doi.org/10.1016/j.jelechem.2010.07.017

Khataee AR, Safarpour M, Zarei M, Aber S (2012) Combined heterogeneous and homogeneous photodegradation of a dye using immobilized TiO_2 nanophotocatalyst and modified graphite electrode with carbon nanotubes. J Mol Catal A Chem 363–364:58–68. https://doi.org/10.1016/j.molcata.2012.05.016

Khataee A, Marandizadeh H, Vahid B, Zarei M, Joo SW (2013) Combination of photocatalytic and photoelectro-Fenton/citrate processes for dye degradation using immobilized N-doped TiO_2 nanoparticles and a cathode with carbon nanotubes: central composite design optimization. Chem Eng Process 73:103–110. https://doi.org/10.1016/j.cep.2013.07.007

Khataee AR, Fathinia M, Zarei M, Izadkhah B, Joo SW (2014) Modeling and optimization of photocatalytic/photoassisted-electro-Fenton like degradation of phenol using a neural network

coupled with genetic algorithm. J Ind Eng Chem 20(4):1852–1860. https://doi.org/10.1016/j.jiec.2013.08.042

Khataee A, Sajjadi S, Hasanzadeh A, Vahid B, Joo SW (2017) One-step preparation of nanostructured martite catalyst and graphite electrode by glow discharge plasma for heterogeneous electro-Fenton like process. J Environ Manag 199:31–45. https://doi.org/10.1016/j.jenvman.2017.04.095

Le TXH, Bechelany M, Lacour S, Oturan N, Oturan MA, Cretin M (2015) High removal efficiency of dye pollutants by electron-Fenton process using a graphene based cathode. Carbon 94:1003–1011. https://doi.org/10.1016/j.carbon.2015.07.086

Le TXH, Bechelany M, Cretin M (2017) Advances in carbon felt material for electro-Fenton process. In: Zhou M, Oturan MA, Sirés I (eds) Electro-Fenton process: new trends and scale-up. Springer, Singapore, pp 145–173. https://doi.org/10.1007/698_2017_55

Li XZ, Zhao BX, Wang P (2007) Degradation of 2,4-dichlorophenol in aqueous solution by a hybrid oxidation process. J Hazard Mater 147(1–2):281–287. https://doi.org/10.1016/j.jhazmat.2006.12.077

Li J, Ai Z, Zhang L (2009) Design of a neutral electro-Fenton system with Fe@Fe_2O_3/ACF composite cathode for wastewater treatment. J Hazard Mater 164(1):18–25. https://doi.org/10.1016/j.jhazmat.2008.07.109

Li H, Lei H, Chen K, Yao C, Zhang X, Leng Q, Wang W (2011) A nano-Fe^0/ACF cathode applied to neutral electro-Fenton degradation of Orange II. J Chem Technol Biotechnol 86(3):398–405. https://doi.org/10.1002/jctb.2530

Li Y, Han J, Mi X, Mi X, Li Y, Zhang S, Zhan S (2017) Modified carbon felt made using $Ce_xA_{1-x}O_2$ composites as a cathode in electro-Fenton system to degrade ciprofloxacin. RSC Adv 7(43):27065–27078. https://doi.org/10.1039/C7RA03302H

Li X, Li H, Li M, Li C, Sun D, Lei Y, Yang B (2018) Preparation of a porous boron-doped diamond/Ta electrode for the electrocatalytic degradation of organic pollutants. Carbon 129:543–551. https://doi.org/10.1016/j.carbon.2017.12.052

Liang L, An Y, Zhou M, Yu F, Liu M, Ren G (2016) Novel rolling-made gas-diffusion electrode loading trace transition metal for efficient heterogeneous electro-Fenton-like. J Environ Chem Eng 4(4):4400–4408. https://doi.org/10.1016/j.jece.2016.10.006

Liang L, Yu F, An Y, Liu M, Zhou M (2017) Preparation of transition metal composite graphite felt cathode for efficient heterogeneous electro-Fenton process. Environ Sci Pollut Res 24(2):1122–1132. https://doi.org/10.1007/s11356-016-7389-3

Lin W-C, Chen C-H, Tang H-Y, Hsiao Y-C, Pan JR, Hu C-C, Huang C (2013) Electrochemical photocatalytic degradation of dye solution with a TiO_2-coated stainless steel electrode prepared by electrophoretic deposition. Appl Catal B 140–141:32–41. https://doi.org/10.1016/j.apcatb.2013.03.032

Liu Y, Chen S, Quan X, Yu H, Zhao H, Zhang Y (2015a) Efficient mineralization of perfluorooctanoate by electro-Fenton with H_2O_2 electro-generated on hierarchically porous carbon. Environ Sci Technol 49(22):13528–13533. https://doi.org/10.1021/acs.est.5b03147

Liu Y, Quan X, Fan X, Wang H, Chen S (2015b) High-yield electrosynthesis of hydrogen peroxide from oxygen reduction by hierarchically porous carbon. Angew Chem Int Ed 127(23):6941–6945. https://doi.org/10.1002/ange.201502396

Liu T, Wang K, Song S, Brouzgou A, Tsiakaras P, Wang Y (2016) New electro-Fenton gas diffusion cathode based on nitrogen-doped graphene@carbon nanotube composite materials. Electrochim Acta 194:228–238. https://doi.org/10.1016/j.electacta.2015.12.185

Luo M, Yuan S, Tong M, Liao P, Xie W, Xu X (2014) An integrated catalyst of Pd supported on magnetic Fe_3O_4 nanoparticles: simultaneous production of H_2O_2 and Fe^{2+} for efficient electro-Fenton degradation of organic contaminants. Water Res 48:190–199. https://doi.org/10.1016/j.watres.2013.09.029

Martínez-Huitle CA, Rodrigo MA, Sirés I, Scialdone O (2015) Single and coupled electrochemical processes and reactors for the abatement of organic water pollutants: a critical review. Chem Rev 115(24):13362–13407. https://doi.org/10.1021/acs.chemrev.5b00361

Moreira FC, Boaventura RAR, Brillas E, Vilar VJP (2017) Electrochemical advanced oxidation processes: a review on their application to synthetic and real wastewaters. Appl Catal B 202:217–261. https://doi.org/10.1016/j.apcatb.2016.08.037

Mousset E, Ko ZT, Syafiq M, Wang Z, Lefebvre O (2016a) Electrocatalytic activity enhancement of a graphene ink-coated carbon cloth cathode for oxidative treatment. Electrochim Acta 222:1628–1641. https://doi.org/10.1016/j.electacta.2016.11.151

Mousset E, Wang Z, Hammaker J, Lefebvre O (2016b) Physico-chemical properties of pristine graphene and its performance as electrode material for electro-Fenton treatment of wastewater. Electrochim Acta 214:217–230. https://doi.org/10.1016/j.electacta.2016.08.002

Mousset E, Wang Z, Hammaker J, Lefebvre O (2017a) Electrocatalytic phenol degradation by a novel nanostructured carbon fiber brush cathode coated with graphene ink. Electrochim Acta 258:607–617. https://doi.org/10.1016/j.electacta.2017.11.104

Mousset E, Weiqi VH, Kai BFY, Koh JS, Tng JW, Wang Z, Lefebvre O (2017b) A new 3D-printed photoelectrocatalytic reactor combining the benefits of a transparent electrode and the Fenton reaction for advanced wastewater treatment. J Mater Chem A 5(47):24951–24964. https://doi.org/10.1039/C7TA08182K

Oturan MA, Aaron J-J (2014) Advanced oxidation processes in water/wastewater treatment: principles and applications. A review. Crit Rev Environ Sci Technol 44(23):2577–2641. https://doi.org/10.1080/10643389.2013.829765

Özcan A, Özcan AA, Demirci Y, Şener E (2017) Preparation of Fe_2O_3 modified kaolin and application in heterogeneous electro-catalytic oxidation of enoxacin. Appl Catal B 200:361–371. https://doi.org/10.1016/j.apcatb.2016.07.018

Pajootan E, Arami M, Rahimdokht M (2014) Discoloration of wastewater in a continuous electro-Fenton process modified graphite electrode with multi-walled carbon nanotubes/surfactant. Sep Purif Technol 130:34–44. https://doi.org/10.1016/j.seppur.2014.04.025

Paz EC, Aveiro LR, Pinheiro VS, Souza FM, Lima VB, Silva FL, Hammer P, Lanza MRV, Santos MC (2018) Evaluation of H_2O_2 electrogeneration and decolorization of Orange II azo dye using tungsten oxide nanoparticle-modified carbon. Appl Catal B 232:436–445. https://doi.org/10.1016/j.apcatb.2018.03.082

Peng Q, Zhao H, Qian L, Wang Y, Zhao G (2015) Design of a neutral photo-electro-Fenton system with 3D-ordered macroporous Fe_2O_3/carbon aerogel cathode: high activity and low energy consumption. Appl Catal B 174–175:157–166. https://doi.org/10.1016/j.apcatb.2015.02.031

Peralta-Hernández JM, Meas-Vong Y, Rodríguez FJ, Chapman TW, Maldonado MI, Godínez LA (2006) In situ electrochemical and photo-electrochemical generation of the Fenton reagent: a potentially important new water treatment technology. Water Res 40(9):1754–1762. https://doi.org/10.1016/j.watres.2006.03.004

Pizzutilo E, Kasian O, Choi CH, Cherevko S, Hutchings GJ, Mayrhofer KJJ, Freakley SJ (2017) Electrocatalytic synthesis of hydrogen peroxide on Au-Pd nanoparticles:from fundamentals to continuous production. Chem Phys Lett 683:436–442. https://doi.org/10.1016/j.cplett.2017.01.071

Plakas KV, Sklari SD, Yiankakis DA, Sideropoulos GT, Zaspalis VT, Karabelas AJ (2016) Removal of organic micropollutants from drinking water by a novel electro-Fenton filter: pilot-scale studies. Water Res 91:183–194. https://doi.org/10.1016/j.watres.2016.01.013

Poza-Nogueiras V, Rosales E, Pazos M, Sanromán MÁ (2018) Current advances and trends in electro-Fenton process using heterogeneous catalysts – a review. Chemosphere 201:399–416. https://doi.org/10.1016/j.chemosphere.2018.03.002

Ramírez J, Godínez LA, Méndez M, Meas Y, Rodríguez FJ (2010) Heterogeneous photo-electro-Fenton process using different iron supporting materials. J Appl Electrochem 40 (10):1729–1736. https://doi.org/10.1007/s10800-010-0157-z

Ramírez G, Recio FJ, Herrasti P, Ponce-de-León C, Sirés I (2016) Effect of RVC porosity on the performance of PbO_2 composite coatings with titanate nanotubes for the electrochemical oxidation of azo dyes. Electrochim Acta 204:9–17. https://doi.org/10.1016/j.electacta.2016.04.054

Recio FJ, Herrasti P, Sirés I, Kulak AN, Bavykin DV, Ponce-de-León C, Walsh FC (2011) The preparation of PbO_2 coatings on reticulated vitreous carbon for the electro-oxidation of organic pollutants. Electrochim Acta 56(14):5158–5165. https://doi.org/10.1016/j.electacta.2011.03.054

Rezgui S, Amrane A, Fourcade F, Assadi A, Monser L, Adhoum N (2018) Electro-Fenton catalyzed with magnetic chitosan beads for the removal of Chlordimeform insecticide. Appl Catal B 226:346–359. https://doi.org/10.1016/j.apcatb.2017.12.061

Ridruejo C, Alcaide F, Álvarez G, Brillas E, Sirés I (2018) On-site H_2O_2 electrogeneration at a CoS_2-based air-diffusion cathode for the electrochemical degradation of organic pollutants. J Electroanal Chem 808:364–371. https://doi.org/10.1016/j.jelechem.2017.09.010

Rostamizadeh M, Jafarizad A, Gharibian S (2018) High efficient decolorization of reactive red 120 azo dye over reusable Fe-ZSM-5 nanocatalyst in electro-Fenton reaction. Sep Purif Technol 192:340–347. https://doi.org/10.1016/j.seppur.2017.10.041

Roth H, Gendel Y, Buzatu P, David O, Wessling M (2016) Tubular carbon nanotube-based gas diffusion electrode removes persistent organic pollutants by a cyclic adsorption – electro-Fenton process. J Hazard Mater 307:1–6. https://doi.org/10.1016/j.jhazmat.2015.12.066

Shen L, Yan P, Guo X, Wei H, Zheng X (2014) Three-dimensional electro-Fenton degradation of methylene blue based on the composite particle electrodes of carbon nanotubes and nano-Fe_3O_4. Arab J Sci Eng 39(9):6659–6664. https://doi.org/10.1007/s13369-014-1184-6

Siahrostami S, Verdaguer-Casadevall A, Karamad M, Deiana D, Malacrida P, Wickman B, Escudero-Escribano M, Paoli EA, Frydendal R, Hansen TW, Chorkendorff I, Stephens IEL, Rossmeisl J (2013) Enabling direct H_2O_2 production through rational electrocatalyst design. Nat Mater 12:1137–1143. https://doi.org/10.1038/nmat3795

Sirés I, Low CTJ, Ponce-de-León C, Walsh FC (2010) The deposition of nanostructured β-PbO_2 coatings from aqueous methanesulfonic acid for the electrochemical oxidation of organic pollutants. Electrochem Commun 12(1):70–74. https://doi.org/10.1016/j.elecom.2009.10.038

Sirés I, Brillas E, Oturan MA, Rodrigo MA, Panizza M (2014) Electrochemical advanced oxidation processes: today and tomorrow. A review. Environ Sci Pollut Res 21(14):8336–8367. https://doi.org/10.1007/s11356-014-2783-1

Sklari SD, Plakas KV, Petsi PN, Zaspalis VT, Karabelas AJ (2015) Toward the development of a novel electro-Fenton system for eliminating toxic organic substances from water. Part 2. Preparation, characterization, and evaluation of iron-impregnated carbon felts as cathodic electrodes. Ind Eng Chem Res 54(7):2059–2073. https://doi.org/10.1021/ie5048779

Tian J, Olajuyin AM, Mu T, Yang M, Xing J (2016a) Efficient degradation of rhodamine B using modified graphite felt gas diffusion electrode by electro-Fenton process. Environ Sci Pollut Res 23(12):11574–11583. https://doi.org/10.1007/s11356-016-6360-7

Tian J, Zhao J, Olajuyin AM, Sharshar MM, Mu T, Yang M, Xing J (2016b) Effective degradation of rhodamine B by electro-Fenton process, using ferromagnetic nanoparticles loaded on modified graphite felt electrode as reusable catalyst: in neutral pH condition and without external aeration. Environ Sci Pollut Res 23(15):15471–15482. https://doi.org/10.1007/s11356-016-6721-2

Wang Y, Zhao G, Chai S, Zhao H, Wang Y (2013) Three-dimensional homogeneous ferrite-carbon aerogel: one pot fabrication and enhanced electro-Fenton reactivity. ACS Appl Mater Interfaces 5(3):842–852. https://doi.org/10.1021/am302437a

Wang Y, Liu Y, Liu T, Song S, Gui X, Liu H, Tsiakaras P (2014) Dimethyl phthalate degradation at novel and efficient electro-Fenton cathode. Appl Catal B 156–157:1–7. https://doi.org/10.1016/j.apcatb.2014.02.041

Wang Q, Zhou S, Xiao S, Wei F, Zhao X, Qu J, Wang H (2018) Novel perovskite-based composites, $La_{1-x}Nd_xFeO_3$@activated carbon, as efficient catalysts for the degradation of organic pollutants by heterogeneous electro-Fenton reactions. RSC Adv 8(27):14775–14786. https://doi.org/10.1039/C8RA00244D

Xie YB, Li XZ (2006) Interactive oxidation of photoelectrocatalysis and electro-Fenton for azo dye degradation using TiO_2–Ti mesh and reticulated vitreous carbon electrodes. Mater Chem Phys 95(1):39–50. https://doi.org/10.1016/j.matchemphys.2005.05.048

Xu X, Liao P, Yuan S, Tong M, Luo M, Xie W (2013) Cu-catalytic generation of reactive oxidizing species from H_2 and O_2 produced by water electrolysis for electro-Fenton degradation of organic contaminants. Chem Eng J 233:117–123. https://doi.org/10.1016/j.cej.2013.08.046

Yang W, Zhou M, Cai J, Liang L, Ren G, Jiang L (2017) Ultrahigh yield of hydrogen peroxide on graphite felt cathode modified with electrochemically exfoliated graphene. J Mater Chem A 5 (17):8070–8080. https://doi.org/10.1039/C7TA01534H

Yang S, Verdaguer-Casadevall A, Arnarson L, Silvioli L, Čolić V, Frydendal R, Rossmeisl J, Chorkendorff I, Stephens IEL (2018a) Toward the decentralized electrochemical production of H_2O_2: a focus on the catalysis. ACS Catal 8(5):4064–4081. https://doi.org/10.1021/acscatal.8b00217

Yang W, Zhou M, Liang L (2018b) Highly efficient in-situ metal-free electrochemical advanced oxidation process using graphite felt modified with N-doped graphene. Chem Eng J 338:700–708. https://doi.org/10.1016/j.cej.2018.01.013

Zarei M, Khataee AR, Ordikhani-Seyedlar R, Fathinia M (2010) Photoelectro-Fenton combined with photocatalytic process for degradation of an azo dye using supported TiO_2 nanoparticles and carbon nanotube cathode: neural network modeling. Electrochim Acta 55(24):7259–7265. https://doi.org/10.1016/j.electacta.2010.07.050

Zhang X, Fu J, Zhang Y, Lei L (2008) A nitrogen functionalized carbon nanotube cathode for highly efficient electrocatalytic generation of H_2O_2 in electro-Fenton system. Sep Purif Technol 64(1):116–123. https://doi.org/10.1016/j.seppur.2008.07.020

Zhang G, Wang S, Yang F (2012) Efficient adsorption and combined heterogeneous/homogeneous Fenton oxidation of amaranth using supported nano-FeOOH as cathodic catalysts. J Phys Chem C 116(5):3623–3634. https://doi.org/10.1021/jp210167b

Zhang G, Zhou Y, Yang F (2015a) FeOOH-catalyzed heterogeneous electro-Fenton system upon anthraquinone@graphene nanohybrid cathode in a divided electrolytic cell: catholyte-regulated catalytic oxidation performance and mechanism. J Electrochem Soc 162(6):H357–H365. https://doi.org/10.1149/2.0691506jes

Zhang C, Zhou M, Ren G, Yu X, Ma L, Yang J, Yu F (2015b) Heterogeneous electro-Fenton using modified iron–carbon as catalyst for 2,4-dichlorophenol degradation: influence factors, mechanism and degradation pathway. Water Res 70:414–424. https://doi.org/10.1016/j.watres.2014.12.022

Zhang C, Zhou M, Yu X, Ma L, Yu F (2015c) Modified iron-carbon as heterogeneous electro-Fenton catalyst for organic pollutant degradation in near neutral pH condition: characterization, degradation activity and stability. Electrochim Acta 160:254–262. https://doi.org/10.1016/j.electacta.2015.01.092

Zhang Y, Gao M, Wang S-G, Zhou W, Sang Y, Wang X-H (2017) Integrated electro-Fenton process enabled by a rotating Fe_3O_4/gas diffusion cathode for simultaneous generation and activation of H_2O_2. Electrochim Acta 231:694–704. https://doi.org/10.1016/j.electacta.2017.02.091

Zhang Z, Meng H, Wang Y, Shi L, Wang X, Chai S (2018) Fabrication of graphene@graphite-based gas diffusion electrode for improving H_2O_2 generation in electro-Fenton process. Electrochim Acta 260:112–120. https://doi.org/10.1016/j.electacta.2017.11.048

Zhao H, Qian L, Guan X, Wu D, Zhao G (2016) Continuous bulk FeCuC aerogel with ultradispersed metal nanoparticles: an efficient 3D heterogeneous electro-Fenton cathode over a wide range of pH 3−9. Environ Sci Technol 50(10):5225–5233. https://doi.org/10.1021/acs.est.6b00265

Zhao H, Wang Q, Chen Y, Tian Q, Zhao G (2017) Efficient removal of dimethyl phthalate with activated iron-doped carbon aerogel through an integrated adsorption and electro-Fenton oxidation process. Carbon 124:111–122. https://doi.org/10.1016/j.carbon.2017.08.034

Zhao H, Qian L, Chen Y, Wang Q, Zhao G (2018a) Selective catalytic two-electron O_2 reduction for onsite efficient oxidation reaction in heterogeneous electro-Fenton process. Chem Eng J 332:486–498. https://doi.org/10.1016/j.cej.2017.09.093

Zhao K, Su Y, Quan X, Liu Y, Chen S, Yu H (2018b) Enhanced H_2O_2 production by selective electrochemical reduction of O_2 fluorine-doped hierarchically porous carbon. J Catal 357:118–126. https://doi.org/10.1016/j.jcat.2017.11.008

Zhou L, Zhou M, Hu Z, Bi Z, Groenen Serrano K (2014) Chemically modified graphite felt as an efficient cathode in electro-Fenton for *p*-nitrophenol degradation. Electrochim Acta 140:376–383. https://doi.org/10.1016/j.electacta.2014.04.090

Zhou M, Oturan MA, Sirés I (eds) (2018) Electro-Fenton process: new trends and scale-up. The handbook of environmental chemistry, vol 61, 1st edn. Springer, Singapore. https://doi.org/10.1007/978-981-10-6406-7